AGU PUBLICATIONS

Reviews of Geophysics

REVIEW ARTICLE

10.1002/2014RG000460

Key Points:
- Explanation of Western Disturbances dynamics with modeling efforts
- Interaction of Western Disturbances with Indian summer monsoon
- Increased frequency of Western Disturbances in recent climate change

Correspondence to:
A. P. Dimri,
apdimri@hotmail.com

Citation:
Dimri, A. P., D. Niyogi, A. P. Barros, J. Ridley, U. C. Mohanty, T. Yasunari, and D. R. Sikka (2015), Western Disturbances: A review, *Rev. Geophys.*, *53*, 225–246, doi:10.1002/2014RG000460.

Received 18 DEC 2014
Accepted 16 MAR 2015
Accepted article online 8 APR 2015
Published online 19 MAY 2015

Western Disturbances: A review

A. P. Dimri[1], D. Niyogi[2], A. P. Barros[3], J. Ridley[4], U. C. Mohanty[5], T. Yasunari[6], and D. R. Sikka[7]

[1]School of Environmental Sciences, Jawaharlal Nehru University, New Delhi, India, [2]Earth, Atmospheric, and Planetary Sciences, Purdue University, West Lafayette, Indiana, USA, [3]Civil and Environmental Engineering, Duke University, Durham, North Carolina, USA, [4]Office Hadley Centre, Exeter, UK, [5]Earth Ocean and Climate Sciences, Indian Institute of Technology, Bhubaneswar, India, [6]Research Institute for Humanity and Nature, Kyoto, Japan, [7]Mausam Vihar, New Delhi, India

Abstract Cyclonic storms associated with the midlatitude Subtropical Westerly Jet (SWJ), referred to as Western Disturbances (WDs), play a critical role in the meteorology of the Indian subcontinent. WDs embedded in the southward propagating SWJ produce extreme precipitation over northern India and are further enhanced over the Himalayas due to orographic land-atmosphere interactions. During December, January, and February, WD snowfall is the dominant precipitation input to establish and sustain regional snowpack, replenishing regional water resources. Spring melt is the major source of runoff to northern Indian rivers and can be linked to important hydrologic processes from aquifer recharge to flashfloods. Understanding the dynamical structure, evolution-decay, and interaction of WDs with the Himalayas is therefore necessary to improve knowledge which has wide ranging socioeconomic implications beyond short-term disaster response including cold season agricultural activities, management of water resources, and development of vulnerability-adaptive measures. In addition, WD wintertime precipitation provides critical mass input to existing glaciers and modulates the albedo characteristics of the Himalayas and Tibetan Plateau, affecting large-scale circulation and the onset of the succeeding Indian Summer Monsoon. Assessing the impacts of climate variability and change on the Indian subcontinent requires fundamental understanding of the dynamics of WDs. In particular, projected changes in the structure of the SWJ will influence evolution-decay processes of the WDs and impact Himalayan regional water availability. This review synthesizes past research on WDs with a perspective to provide a comprehensive assessment of the state of knowledge to assist both researchers and policymakers, and context for future research.

1. Introduction

The Himalayas, due to their unique geographical position, provide a physical barrier that plays an important role in global weather patterns (Figure 1) by acting as a heat source during the summer and a heat sink during the winter. Topographic heterogeneity, land use variability, and varying snow cover extent are important climate controls of the Indian Summer Monsoon (ISM) [*Boos and Kuang*, 2010]. During winter, the Himalayan region is prone to severe weather due to large amounts of snowfall produced by Western Disturbances (WDs). Snowfall in the central Himalayas occurs during southward excursions of the Subtropical Westerly Jet (SWJ) [*Schiemann et al.*, 2009] associated with terrain-locked, low pressure systems (WDs) at the notch formed by the Himalayas and the Hindu Kush Mountains [*Lang and Barros*, 2004]. Regional spring snowmelt runoff contributes 15–44% of the discharge to the tributaries of the Indus and 6–20% of the Ganges discharge [*Ramasastri*, 1999]. Spring runoff becomes especially important in the case of delayed monsoon onset [*Bamzai and Shukla*, 1999; *Liu and Yanai*, 2002] and is a factor in premonsoon flooding and landslides [*Agrawal*, 1999; *Thayyen et al.*, 2012].

The intune relationship between Eurasian snow cover and the associated albedo and the strength of the following ISM is well documented in the literature [*Vernekar et al.*, 1995; *Dash et al.*, 2004, 2005; *Mamgain et al.*, 2010]. *Bhattacharya et al.* [2011] reported a decreasing trend in the mean and the variability of surface albedo over India between 1981 and 2000. In particular, interannual albedo variability due to changes in the Himalayan snow cover exhibits a prominent decline. This trend was attributed to increasingly earlier beginning of the snow melting season and increase of snowmelt source areas. A recent weakening of the El Niño–Southern Oscillation (ENSO)-ISM relationship [*Kucharski et al.*, 2007] suggests an increased role of the regional, interannual variability of the ISM that has not yet been detected in the context of wintertime Himalayan snow cover [*Krishna Kumar et al.*, 1999, 2006; *Saha et al.*, 2011]. The mass balance of glaciers in the northwestern Himalayas is intimately dependent upon winter precipitation [*Bolch et al.*, 2012], and

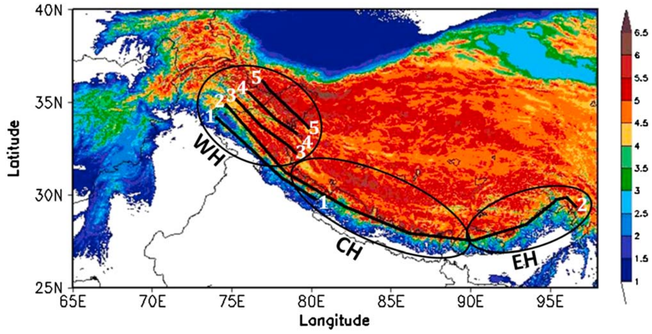

Figure 1. Schematic representation of cascading Himalayan mountain ranges (marked in black colors as 1-1: Pir Panjal, 2-2: Great Himalaya, 3-3: Zanskar, 4-4: Ladhak, and 5-5: Karakoram) over Western Himalayas (WH), Central Himalayas (CH), and Eastern Himalayas (EH) (elongated circles with corresponding marking, respectively) with topographic height (in km, shaded) in an overview of the Himalayas.

natural hazards including landslides, avalanches, and floods can be directly traced to these winter storms and associated precipitation [*Rangachary and Bandyopadhyay*, 1987; *Ganju and Dimri*, 2004; *Das et al.*, 2006; *Srinivasan et al.*, 2005; *Thayyen et al.*, 2012]. Further, in the context of precipitation forming mechanisms and in conjunction with complex topography, very little was known until *Smith's* [1979] classic review, which has been recently updated by *Houze* [2012].

A fundamental understanding of the dynamics of WDs is therefore essential not only to short-term and seasonal hydrometeorological forecasting but also to the assessment of regional climate change and its impacts. The objective of this manuscript is to provide a synthesized overview of the state of knowledge on WDs in the context of prior and current research.

2. WDs: Synoptic Scale

The first long-term weather forecasts, using the link between the nature of snowfall and accumulation patterns in the Himalayas and rainfall in the rest of India, were conducted after the establishment of the India Meteorological Department in 1875 [*Blanford*, 1884]. The problem of Long Range Forecasting of ISM rainfall has been one of the major tasks of Indian meteorologists for more than a century [*Blanford*, 1884; *Walker*, 1924; *Montgomery*, 1940].

Flohn [1968] was the first to uncover the significance of the high Tibetan region in defining the role of wind using a limited set of available in situ observations. Over the western mountains and valleys, the largest portion of rainfall is produced by propagating disturbances of the westerlies (mainly upper level troughs) during winter. This is a unique climatic feature that has been inadequately treated in textbooks related to regional climatology. To study this winter weather phenomena, *Venkiteshwaran* [1939] relied on a simple sounding balloon at Agra (near New Delhi, India) to discuss a synoptic weather system during the winter of 1931, referring to it as a "Winter Disturbance." An analysis of the relative positions of the tropical and extratropical depressions provided the first systematic analysis to predict wet and dry disturbances and introduced the terminology "Western Disturbance" for the first time in published literature [*Malurkar*, 1947].

The origin and structure of western depressions over northwest India were initially described and classified as "weak" extratropical disturbances, traveling with the narrow but intense jet stream that flows around the southern rim of the Indian Himalayas [*Mull and Desai*, 1947; *Riehl*, 1962]. The moisture in these storms usually originates over the Mediterranean Sea and the Atlantic Ocean. Extratropical storms are a global rather than a localized phenomenon with moisture usually carried in the upper atmosphere and localized behavior such as frontal systems. Primarily, interaction of air masses with different characteristics leads to formation of discontinuity surfaces called frontal systems. Winter WDs are thus similar to the Bjerknes cyclones of the Pacific and Atlantic because of the asymmetric upper air trough having closer packing of isobars at the rear of the formation (Figure 2) [*Pisharoty and Desai*, 1956] than at the leading edge. In the following section, the northwesterly shift of the packing associated with WDs from the surface to the upper atmosphere is demonstrated with the help of results from recent modeling studies.

Pisharoty and Desai [1956] explained that heavy rainfall over the eastern Himalayan region was a result of the interaction of WDs with a break in the summer monsoon trough. Examining a decade-long (1945–1955) precipitation record over the Indian subcontinent, *Mooley* [1957] systematically classified synoptic situations across the Himalayan region. In contrast to *Pisharoty and Desai* [1956], Mooley suggested that WDs differ from extratropical depressions in that they generally do not always have well-marked cold or warm fronts

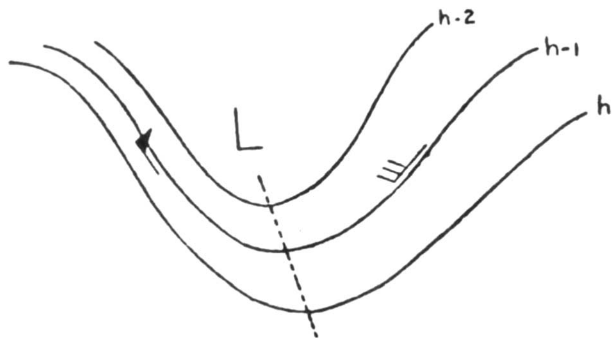

Figure 2. A schematic representation of asymmetric upper air (200 hPa) trough and wind (knots) with closer packing in the rear; *h* corresponds to geopotential heights. Source: *Pisharoty and Desai* [1956].

either at the surface or upper levels and concluded that orographic convergence plays a leading role in the production of localized heavy rain [*Dimri and Niyogi*, 2012]. This explanation added clarification to the presence of extratropical cyclones in the midlatitude westerlies.

In showing that WDs are preceded by warm and moist air from southern latitudes and succeeded by cold and dry air from northern latitudes, *Mooley* [1957] provided the first evidence linking the occasional presence of WDs during summertime with intensification of the ISM. Interlocking/merging of WD lows with the Intertropical Convergence Zone associated with the ISM invigorates the monsoon flow. Although Mooley's study examined various facets of the WD structure, its interactions with Himalayan topography and the ISM among other interactions, it did not provide a full description of the underlying dynamics. This was achieved by *Singh* [1963] with an in-depth study of a WD that was observed on 28–31 December 1960. The Singh study examined WD vertical structure, evolution and decay, and associated jet stream movement. The analysis revealed that the vertical structure of WDs is determined by two synoptic components, an upper level trough and a lower level cyclonic circulation: extratropical cyclones march eastward with the upper level trough in the SWJ and move over and subsequently become linked to existing stationary low-level cyclonic circulations forming a WD [*Dimri and Chevuturi*, 2013].

Ramaswamy [1966] analyzed WDs based on the principle of conservation of vorticity and related dynamics, which changed the ongoing and established practice of forecasters relying on delineation of frontal systems at the synoptic scale. Further characterization of WDs by *Datta and Gupta* [1967] indicated that they move at a speed of 8 to 10° longitude per day (e.g., 10–12 m s^{-1}) except during the formation and dissipation stages when the movement is comparatively slow with a life-cycle duration of 3–4 days.

Chakravarti [1968a, 1968b] advanced two important insights related to synoptic characteristics of the WDs. First, he stipulated the governing role of the Indian Himalayas in WD dynamics, and second, he noted that WDs that lead to precipitation are initially generated and travel in upper atmospheric flow patterns. As an increasing number of ground and upper air observations became available, the India Meteorological Department (IMD) published its first manual to guide forecast analysis at the synoptic scale [*Rao and Srinivasan*, 1969]. *Singh and Kumar* [1977] established that a well-organized upper tropospheric frontal layer in the westerlies over a preexisting surface low is essential for WD development. The upper level front propagates eastward in association with an upper air trough, and the growth of the upstream ridge is one of the key mechanisms that creates a deep trough downstream [*Singh et al.*, 1981]. As a result, on a climatological basis, about four to six intense WDs occur during the winter months from November to March [*Mohanty et al.*, 1998]. The annual frequency of snowstorms is consistent with WD frequency [*Lang and Barros*, 2004], and heavy precipitation is persistent through the average 2–3 day WD life cycle over the western Himalayas.

3. WDs: Linkage With the Jet Stream

The upper level flow over the Tibetan Plateau responds to the Asian continent's mechanical and thermodynamical forcing and feedbacks [*Academica Sinica*, 1957; *Webster et al.*, 1998; *Yanai et al.*, 1992; *Wu and Liu*, 2003; *Duan and Wu*, 2005]. In turn, the position of the jet stream over central Asia affects WD evolution in multiple and nonlinear ways that continue to be both interesting and challenging to study. However, the role of the jets in controlling winter weather was poorly understood until radiosonde observations revealed the presence of a quasi-permanent SWJ over the Indian subcontinent from October to May [*Koteswaram et al.*, 1953; *Koteswaram and Parathasarathy*, 1954]. A surge in studies of jet stream dynamics was enabled by increased availability of upper air soundings from the 1950s to the 1970s

[*Chaudhury*, 1950; *Murray*, 1953; *Mohri*, 1953, 1958; *Riehl et al*., 1954; *Bannon*, 1954; *Endlich and McLean*, 1957; *Defant and Taba*, 1957, 1958; *Newton and Persson*, 1962; *Serebreny et al*., 1962].

In the context of Indian weather, the role of the SWJ in premonsoon large-scale convection was elucidated by *Ramaswamy* [1956], which led to significant advances in thunderstorm predictability. In a subsequent study, *Ramaswamy* [1962] demonstrated the interaction of the tropical easterly jet (TEJ) and the SWJ to define gaps and active conditions during the ISM. Knowledge of the day-to-day positioning of the TEJ and SWJ proved invaluable for prognostic evaluation of Indian weather [*Koteswaram*, 1957a, 1957b]. In winter, the polar front jet, located at 43°N, can merge with the SWJ [*Singh*, 1971]. This confluence forces the SWJ to move northward, allowing the southward migration of cold and dry polar air from the north. The temperature gradient intensifies and builds to a quasi-SWJ with an elongated wind structure that can extend throughout the troposphere. An analysis of temperature at three tropospheric pressure levels revealed two dynamic zones over western and central India at 25°N and at 33°N, respectively [*Singh*, 1980]. The southern zone is formed by the meeting of a tropical air mass with a midlatitude air mass, coinciding with the axes of WDs [*Dimri and Chevuturi*, 2013]. Furthermore, the evolution of an upper tropospheric temperature structure over the Middle East and synoptic predictability of the behavior of the jet stream helps in defining its southern zone over India. Thus, seasonal meridional translation/progression of the SWJ could be a good index for the determination of the WDs and associated seasonal patterns [*Bugayev et al*., 1957; *Academica Sinica*, 1957; *Chanysheva et al*., 1995].

Schiemann et al. [2009] characterized the SWJ over the Tibetan Plateau region highlighting a pronounced seasonal cycle. During peak winter months (December–April), WDs have a significant presence over northern India and the SWJ is positioned over the southern edge of the Tibetan Plateau. Also, monthly mean horizontal wind speed intensity is strongest in winter and decreases in spring. A modest variation in the latitudinal positioning of the SWJ over the Himalayas can modulate the incoming stationary wave flux from middle and high latitudes [*Nigam and Lindzen*, 1989] and therefore remotely impact atmospheric dynamics. There are studies using contemporary reanalysis data that further establish a relationship between the SWJ intensity and baroclinic wave activity over the northern Atlantic Ocean [*Nakamura*, 1992] as well as a relationship between the seasonal cycle of the SWJ with a meridional temperature gradient in the upper troposphere [*Kuang and Zhang*, 2005].

4. WDs: Satellite-Based Analysis

Access to satellite imagery changed the tools and methodologies of weather forecasting and further elucidated the multiscale features associated with WDs [*Houghton*, 1987]. The first synoptic charts with input from satellite imagery showing jets and cloud systems for India were produced in 1970 [*Srinivasan*, 1971]. Satellite imagery was also used to analyze the cloud bands associated with WDs, classifying cloud patterns in terms of the relationship between geometry and cloud area [*Rao and Moray*, 1971]. Such structure-based cloud imageries helped in assessing the evolution and categorization of WDs [*Agnihotri and Singh*, 1982]. Analysis of satellite imagery identified the presence of secondary extratropical depressions traveling with large-scale westerlies and approaching northwest India. These secondary depressions, being shallow systems that do not extend above 700 hPa, could not be tracked in the synoptic charts and had posed a challenge for forecasters. *Sharma and Subramaniam* [1983] linked these systems to the intensification of the WD and the extension of associated precipitation far into the southern part of India.

A satellite-based relationship between cloud top temperatures and WD rainfall in the relatively drier month of November was proposed by *Veeraraghavan and Nath* [1989]. Another important aspect of the interaction between the tropics and midlatitudes that has become clearer is the emergence of cloud surges caused by the interaction of tropical and midlatitude baroclinic flows over the region. When the existence of large-amplitude troughs in the subtropical westerlies impinge upon low-latitude synoptic disturbances, signatures of cloud deformation extending northeastward from the lower latitudes can be observed in the satellite data [*Kalsi and Halder*, 1992]. Such interactions during the summer monsoon months further enhance monsoonal flow. Presently, satellite observations from multiple platforms are routinely used to delineate cold air intrusion and atmospheric moisture patterns and thus monitor the life cycle of WDs [e.g., *Puranik and Karekar*, 2009].

Table 1. The Progression of Modeling Efforts on Western Disturbances With Significant Findings[a]

Reference	WD Case Discussed	Model Used	Horizontal Model Resolution	Parameterization Schemes: Convective	Parameterization Schemes: PBL	Significant Findings
Rao and Rao [1971]	11–17 Dec 1963	Observational data used				The WD development shows similar characteristics to a baroclinically unstable disturbance.
Ramanathan and Saha [1972]	22–25 Dec 1968; 11–14 Jan 1969	Primitive equation limited-area barotropic model	2.5°			Forecasts of WD with the limited area model could generally predict the movement of the WD but need to improve resolution and reduce forecast error.
Chitlangia [1976]	4–5 Jan 1959; 3–4 Feb 1959; 20–21 Jan 1962; 25–26 Jan 1962; 23–24 Feb 1962; 19–20 Jan 1965	Moving coordinate system (empirical model)	1°			During a WD, the vertical structure of atmosphere shows more complex characteristics than an extratropical depression with a simple two-layer model.
Dash and Chakrapani [1989]	27 Feb to 3 Mar 1982	Global spectral model (Indian Institute of Technology Delhi)				The forecast fields of 24 h accumulated precipitation and wind circulation patterns show agreement with the respective analysis.
Gupta et al. [1999]	27–30 Dec 1994; 8–10 Jan 1995; 15–17 Jan 1996; 19–21 Jan 1997	NCEP T80, 18-layer global spectral model (National Centre for Medium Range Weather Forecasting)	160 km			The model is able to forecast intensity and extent of winter systems 72 h in advance but not able to provide point specific predictions.
Azadi et al. [2001]	18–21 Jan 1997	MM5 (V2.12)	60 km	Kuo, Grell, Kain-Fritsch, Betts-Miller	Blackadar and Hong-Pan	Hong-Pan PBL scheme and Betts-Miller cumulus scheme give better results compared to the other parameterization schemes.
Das [2002]	14–16 Sep 2001	MM5	90 km, 30 km, and 10 km	Grell	Hong-Pan	Results show that model forecasts of WD and associated wind and precipitation compare well with observations over the region.
Das et al. [2003]	14–16 Sep 2001	MM5	90 km, 30 km, and 10 km	Grell	Hong-Pan	Model forecasts and WD features are well depicted 72 h in advance of the system.
Dimri [2004]	21–25 Jan 1999	MM5 (V2.12)	90 km, 60 km, and 30 km	Betts-Miller	Hong-Pan	Better representation of topographical features in the finer domain leads to improved simulation of the WD and associated precipitation.
Dimri et al. [2004]	21–25 Jan 1999	MM5 (V2.12)	60 km	Betts-Miller	Hong-Pan	Model simulation captured the movement and intensity of the WD along with representing some fine structure not observed in the verification analysis.
Dimri et al. [2006]	18–21 Jan 1997; 20–25 Jan 1999	MM5 (V2.12)	90 km, 60 km, and 30 km	Kuo, Grell, Kain-Fritsch, and Betts-Miller	Blackadar and Hong-Pan	Sensitivity analysis suggests that WD simulation is better represented with a combination of the Hong-Pan PBL scheme and Betts-Miller convective scheme and finer horizontal model resolution.

Table 1. (continued)

Reference	WD Case Discussed	Model Used	Horizontal Model Resolution	Parameterization Schemes		Significant Findings
				Convective	PBL	
Hatwar et al. [2005]	13–17 Jan 2002; 5–8 Feb 2002	IMD limited area analysis forecast system	1°	Model description in detail in *Krishnamurti et al.* [1990]	Precipitation patterns in the forecast compare well with the verification analysis, but the intensity of rainfall is underpredicted in the model output.	
Azadi et al. [2005]	24 Mar 1993; 14 Feb 1995; 15 Jan 1996; 12 Mar 1998	MM5 (V2.12)	90 km, 60 km, and 30 km	Betts-Miller	Hong-Pan	Model-simulated synoptic system and associated features compare well with the analysis but shows a slight bias which slows the system.
Das et al. [2006]	14–16 Jan 2002	MM5	90 km, 30 km, and 10 km	Grell	Hong-Pan	Forecasts up to 72 h show good capability of the model to predict rainfall over the mountainous regions.
Srinivasan et al. [2005]	13–15 Mar 2001; 13–17 Jan 2002; 16–20 Feb 2003	MM5 model (integrated with snow cover model and statistical model)	30 km			Improved avalanche prediction was observed on application of model-predicted meteorological parameters.
Semwal and Giri [2007]	30 Dec 2004 to 04 Jan 2005; 3–7 Feb 2007	ARPS (V5.1.5)	30 km	Kain-Fritsch		Model simulates spatial distribution of the precipitation well and shows heterogeneous precipitation distribution on comparison with observation analysis in cases of merging WDs.
Dimri and Mohanty [2009]	17–20 Jan 1997; 1–4 Feb 1997; 8–11 Feb 1997; 23–26 Feb 1997	MM5 (V2.12)	60 km	Betts-Miller	Hong-Pan	Model simulations of active WDs represent the associated mesoscale features well.
Hara et al. [2004]	27–31 Dec 1990	RAMS	100 km			A simulation of a quasi-stationary cyclone over the southern slope of the Himalayas is depicted as a topographic Rossby wave.
Semwal and Dimri [2012]	1–4 Jan 2006; 31 Dec 2004 to 03 Jan 2005; 3–6 Feb 2005	ARPS (V5.1.5)	30 km and 10 km	Kain-Fritsch		Complex topography and local meteorological effects impact the prediction of heterogeneous precipitation distribution.
Rakesh et al. [2009]	8–11 Feb 2007	MM5 using 3DVar assimilation (with MODIS-derived data)				Forecast initialization with 3DVar approach shows improved results over the simulation without incorporation of MODIS satellite data sets.
Dasgupta et al. [2012]	23 Apr 2004	MM5 (V3.4) using 3DVar assimilation	90 km, 30 km, and 10 km	Grell	Nonlocal closure scheme	Improvement of precipitation forecasts is observed in simulation with 3DVar assimilation.
Dimri and Niyogi [2012]	1980–2001	RegCM3	60 km and 10 km	Grell	Holtslag	Model dynamical downscaling captures the topography and precipitation interaction well with finer resolution showing better results over WH.

Table 1. (continued)

Reference	WD Case Discussed	Model Used	Horizontal Model Resolution	Parameterization Schemes		Significant Findings
				Convective	PBL	
Dimri et al. [2013]	1990–2007	HadRM3 and REMO	0.23° (~25 km)	Mass flux of *Gregory and Rowntree* [1990] and mass flux of *Tiedtke* [1989]		Regional climate models captured features of dynamic and orographic forcing along with the associated precipitation mechanisms of WDs.
Thomas et al. [2013]	17–18 Feb 2003; 21–22 Jan 2003; 10–11 Feb 2007; 27–28 Feb 2007; 11–12 Mar 2007	WRF (ARW)	45 km and 15 km	Grell Devenyi ensemble	Yonsei University (YSU)	For WDs simulations with ARW, RUC land surface parameterization is best suited.
Dimri and Chevuturi [2013]	13–17 Jan 2002; 5–8 Feb 2002; 11–13 Feb 2002	WRF (ARW)	81 km, 27 km, and 9 km	Kain-Fritsch	Yonsei University (YSU)	Eta grid-scale cloud and precipitation microphysics scheme, Yonsei University scheme, and Kain-Fritsch scheme are found to be the best suite for WD studies over the Himalayan region.

[a]PBL, planetary boundary layer; NCEP, National Centers for Environmental Prediction; MM5, Mesoscale Model 5; ARPS, Advanced Regional Prediction System; RAMS, Regional Atmospheric Modeling System; 3DVar, three-dimensional variational; MODIS, Moderate Resolution Imaging Spectroradiometer; RegCM3, Regional Climate Model version 3; HadRM3 and REMO, Hadley Center Regional Climate Model version 3 and Max Planck Institute of Meteorology Regional Climate Model; WRF, Weather Research and Forecasting; ARW, Advanced Research Workshop; RUC, Rapid Update Cycle.

5. WDs: Diagnostics

To determine the energy and water budgets of large-scale synoptic systems, a variety of diagnostic process studies are required. The kinetic energy budget is diagnosed from meridional and zonal flow. In WDs, the adiabatic kinetic energy generation due to enhanced meridional flow is consumed by zonal flow along its track [*Ananthakrishnan and Keshavmurty*, 1973]. *Gupta and Mandal* [1987] explained the behavior of the kinetic energy generation function during a WD. Their study revealed that the increase or decrease in the kinetic energy content of the system could not be related directly to the positive or the negative contribution of the kinetic energy generation function. Further, the zonal component of the kinetic energy generation function acted as a source, while the meridional component behaved as a strong sink in the upper levels throughout the life cycle of the system. Despite data paucity in the Himalayas, reanalysis products depict the characteristics of the large-scale circulation of WDs reasonably well [*Mohanty et al.*, 1998, 1999]. For example, *Roy and Bhowmik* [2005] were successful in revealing the advection of water vapor over Delhi as a consequence of the passage of WDs by using models and reanalysis. The role of the Himalayan orography acts in blocking and guiding the integrated moisture fluxes approaching from the western Mediterranean region and/or the Arabian Sea. In reanalysis fields, strong moisture flux convergence and adiabatic production of kinetic energy is seen over northern India during the passage of a WD [*Raju et al.*, 2011], who confirmed the earlier findings of *Ananthakrishnan and Keshavmurty* [1973]. These diagnostic studies have provided insight on energy distribution during the course of WD evolution and decay.

6. WDs: Modeling Efforts

A survey of modeling efforts of WD events with a focus on significant milestones is described in this section. Table 1 presents the dynamical framework typically associated with the different modeling studies.

The first mathematical description of cyclonic waves in the baroclinic westerlies was introduced by *Charney* [1947] and provided a theoretical basis for numerical weather prediction [*Charney*, 1948; *Charney et al.*, 1950]. Here we mainly rely on the existing dynamical numerical models of WDs. *Rao and Rao* [1971] considered that the observed zonal wind profile is unstable with respect to a small superimposed disturbance, most notably for a perturbation wavelength of around 7000 km at 28°N. Such baroclinic instability is a possible mechanism for energy release and WD development. *Ramanathan and Saha* [1972] applied a primitive equation

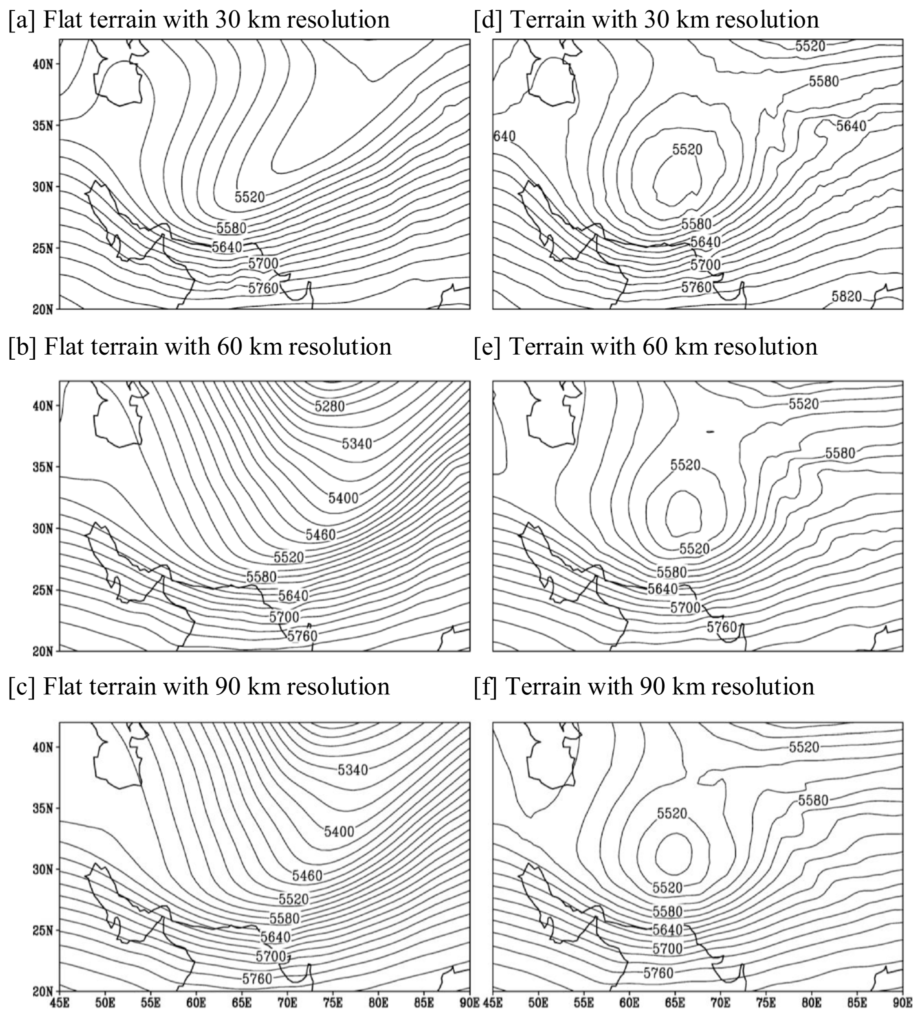

Figure 3. On 23 January 1999, 500 hPa geopotential height (m) after 48 h model forecast valid at 0000 UTC over flat topography with (a) 30 km, (b) 60 km, and (c) 90 km horizontal model resolution. (d–f) Same as Figures 3a–3c but with normal model topography. Source: *Dimri* [2004].

barotropic model at 500 hPa to predict WD evolution, investigated the role of initial and boundary conditions on forecast skill, and reported encouraging and important applications of dynamical models to predict WD movement. *Chitlangia* [1976] employed a moving coordinate system to study the mean structure of a WD and provided an estimate of its future state based on purely empirical methods. *Hoskins and Karoly* [1982] used a steady state-linearized, five-layer baroclinic model to establish how subtropical forcings could produce an appreciable response in middle and high latitudes. In low latitudes, the Hoskins-Karoly model establishes that longer wavelengths propagate poleward and eastward, whereas shorter wavelengths are trapped near the equator side of the jet. This trapped jet enhances the evolution of embedded WDs. *Nigam and Lindzen* [1989] and *DeSilva and Lindzen* [1993] investigated stationary waves in the Northern Hemisphere winter using stationary and time-dependent linear primitive equation models. These studies found that small displacements in the SWJ yielded significant changes in the stationary wave's response in the troposphere and the lower troposphere. This behavior has potential for long-range forecasting of synoptic weather systems associated with the SWJ, such as WDs.

Dash and Chakrapani [1989] reported improvements in the forecast skill of geopotential heights, wind magnitude, and precipitation using a global spectral model to simulate a WD event for the first time. As numerical weather prediction (NWP) models continued to evolve over the last three decades, further improvements in the predictability of precipitation associated with WDs have been associated with the introduction and testing of parameterizations of boundary layer and convective processes in NWP models.

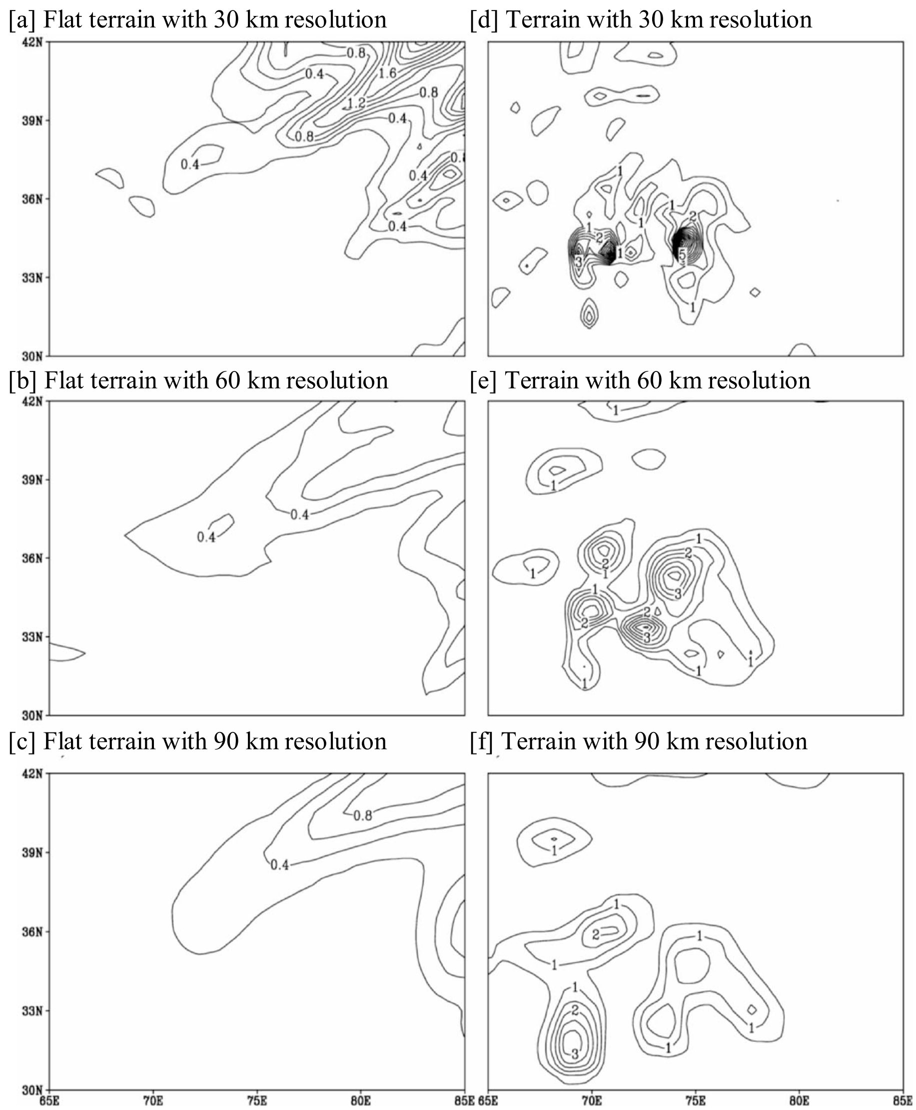

Figure 4. Precipitation (mm/d) after 48 h model forecast valid at 0000 UTC on 23 January 1999 over flat topography with (a) 30 km, (b) 60 km, and (c) 90 km horizontal model resolution. (d–f) Same as Figures 4a–4c but with normal model topography. Source: *Dimri* [2004].

An investigation of multiple combinations of parameterization of physical processes for capturing the dynamical structure of WDS was conducted first by *Azadi et al*. [2001] using the MM5V3 (Mesoscale Model 5 Version 3) to simulate the 18–19 January 1997 WD event. Simulations for different combinations of planetary boundary layer and cumulus parameterization schemes are shown in with modeling experiment. In this experiment, evolution of the WD is seen with eight different combinations of four cumulus parameterization schemes (Kuo, Grell, Kain-Fritsch, and Betts-Miller) and two planetary boundary layer schemes (Blackadar and Hong-Pan). The results show that combination of Betts-Miller and Hong-Pan schemes yields the best model evolution of WD. Model configuration guidance from such studies is necessarily bound to the specific model, model version, and parameterizations available at the time the study was conducted. Because new models become available, and model formulation and implementation as well as physical parameterizations continuously evolve to incorporate scientific and technological advances, benchmark studies for understanding the model physics and dynamics associated with WD simulation should be repeated regularly [*Das et al*., 2003; *Das*, 2005; *Hatwar et al*., 2005; *Dimri and Chevuturi*, 2013].

Dimri [2004] investigated the impact of topography and model resolution on an MM5V3 simulation of a WD event on 23 January 1999 and showed that the WD evolution, in terms of its low pressure at 500 hPa, is

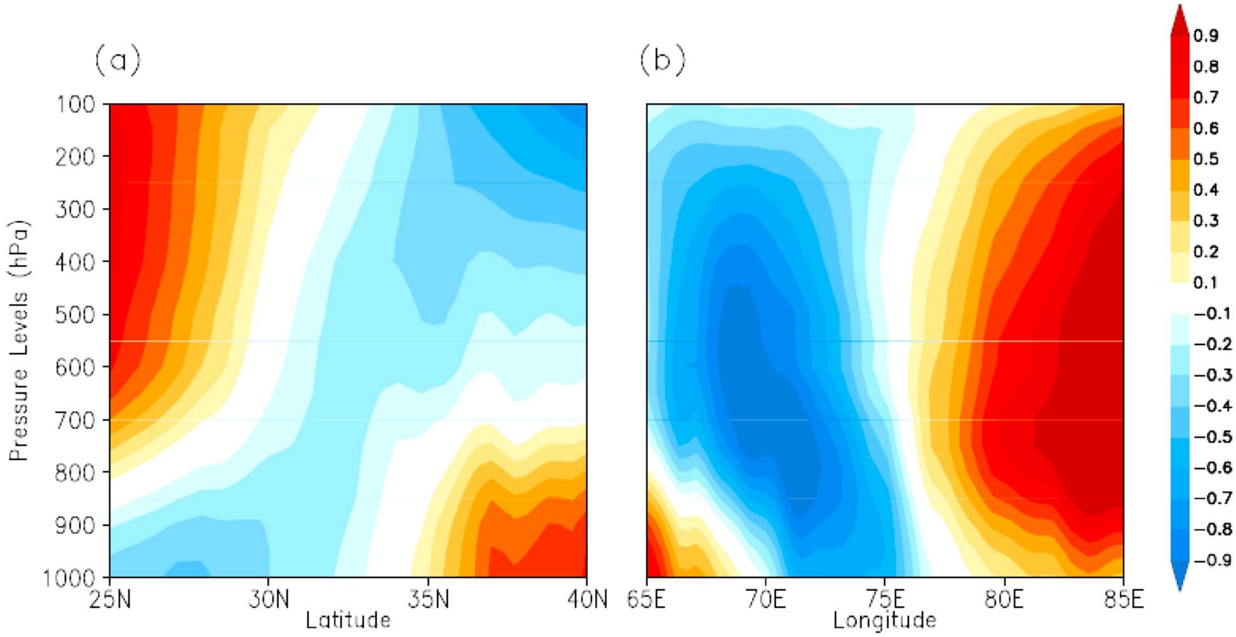

Figure 5. (a) Latitude-pressure distribution of geopotential anomaly (× 100 m) calculated from the average at same pressure level over longitude 65–85°E and (b) longitude-pressure distribution of geopotential anomaly (× 100 m) calculated from the average at same pressure level over latitude 25–40°N on 7 February 2002 0000 UTC.

stronger when realistic topography is present (Figures 3d–3f) than if no topography is introduced (Figures 3a–3c). Unsurprisingly, more organized precipitation fields along the upwind slopes of the Himalayan complex are simulated when the representation of the topography is realistic (Figures 4d–4f) compared to when it is not the case (Figures 4a–4c). *Dimri and Chevuturi* [2013] applied the Weather Research and Forecasting (WRF) modeling framework and analyzed the vertical dynamic structure of the WD during the 5–8 February 2002 event. Figure 5 shows the vertical distribution of a model-simulated geopotential anomaly that occurred on 7 February 2002. The vertical axis of the WD that links the surface low to the upper air depression is notably tilted northwestward from the surface to the upper atmosphere. In the course of the evolution-propagation-demise of the WD, the surface low remains stationary, but the upper air depression moves eastward with the upper level westerlies. Subsequently, the northwestward tilted axis straightens and farther tilts eastward with time. The associated intensification and modulation of the WD are further illustrated in Figure 6a, where results of WRF model simulations for the WD event on 7 February 2002

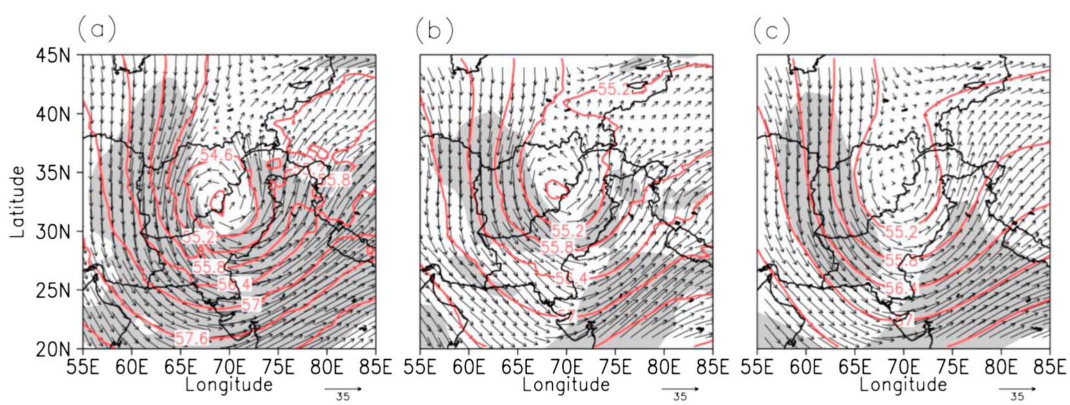

Figure 6. 500 hPa wind (m/s; arrow); geopotential height (× 100 m; red contour) and wind speed above 22 m/s (grey shading) in (a) WRF model (source: *Dimri and Chevuturi* [2013]), (b) Modern Era Retrospective Analysis for Research and Applications (MERRA) [*Rienecker et al.*, 2011], and (c) National Center for Environmental Prediction-National Center for Atmospheric Research Reanalysis II Project (NCEP-NCARII) reanalysis products [*Kanamitsu et al.*, 2002] on 7 February 2002 0000 UTC. Figure 6a corresponds with Figure 5.

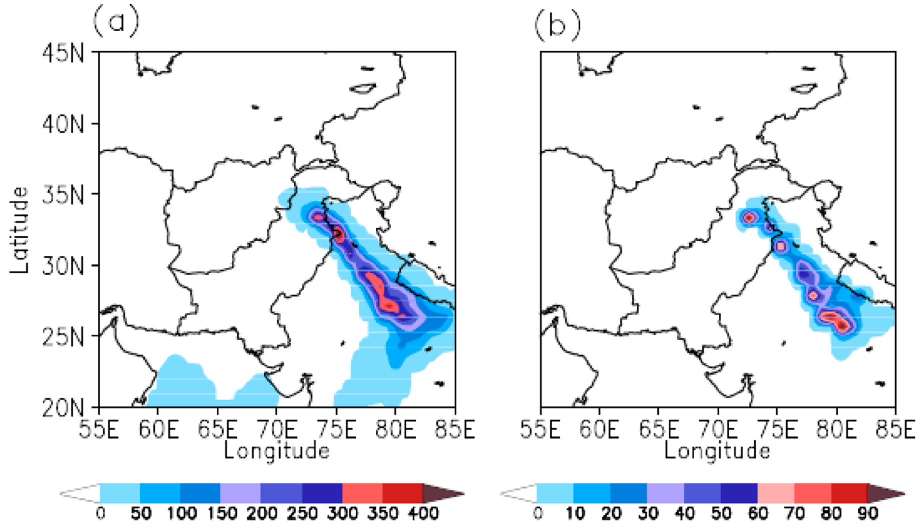

Figure 7. Spatial distribution of WRF model simulated maximum (a) CAPE (J/kg) and (b) CIN (J/kg) on 7 February 2002 0000 UTC. Source: *Dimri and Chevuturi* [2013].

were compared against reanalysis products. Figure 6a shows model-simulated 500 hPa wind, geopotential height, and wind speed, with a similar cyclonic structure as in the corresponding Modern Era Retrospective Analysis for Research and Applications (MERRA) [*Rienecker et al.*, 2011] and National Center for Environmental Prediction-National Center for Atmospheric Research Reanalysis II Project (NCEP-NCARII) reanalysis products [*Kanamitsu et al.*, 2002] shown in Figures 6b and 6c. The spatial distributions of thermodynamic indices, such as maximum convective available potential energy (CAPE) and convective instability (CIN), are presented in Figures 7a and 7b. Note the close alignment of CAPE and CIN with the Himalayan topography. These studies consistently highlight the intensification of winter storms and associated precipitation enhancement due to orographic forcing. Such interplay of the WD with topography provides an explanation for the propensity of increased weather activity over northern India [*Dimri and Niyogi*, 2012].

Since Azadi's first study, the sensitivity of simulated WD events to model physics, spatial horizontal model resolution, topography, and domain size has been extensively examined by many, recently by putting emphasis on the characterization of model errors such as systematic bias that increases with integration time [*Dimri and Mohanty*, 2009]. The model biases tend to be reduced to a certain extent through the assimilation of satellite-derived atmospheric temperature profiles [*Rakesh et al.*, 2009], surface observations [*Dasgupta et al.*, 2012], and improved boundary conditions such as land use maps [*Thomas et al.*, 2013]. The combination of updated model physics and data assimilation has provided an opportunity for improving the simulated precipitation intensity and dynamics associated with a WD's dynamical evolution for operational forecasting. Improved understanding of modeling strategies has in recent decades enabled the simulation and prediction of WD structure and dynamics with a level of detail and accuracy that was previously elusive to forecasters [*Srinivasan et al.*, 2005].

7. WDs: Orography and Land-Atmosphere Interactions

The interplay of WDs with the topography of the western Himalayas determines the spatial and vertical distribution of precipitation. The annual precipitation pattern derived from the Tropical Rainfall Measuring Mission satellite data shows gradients across the Himalayan range, from east to west, and fivefold differences between major valleys and their adjacent ridges [*Barros et al.*, 2000; *Lang and Barros*, 2002; *Anders et al.*, 2006]. The interannual variability of precipitation in the Nepal region of the Himalayas is dependent on the timing of the summer monsoon onset along the Himalayan range and is linked to the trajectory and strength of the monsoon depressions forming over the Bay of Bengal [*Lang and Barros*, 2002; *Barros et al.*, 2006]. The precipitation to cloudiness scaling suggests a strong stationary behavior of orographic land-atmosphere interactions based on elevation class and ridge-valley scales [*Barros et al.*, 2004]. This is to be expected as topography plays a crucial role in modifying storm systems, including WDs [*Dimri*, 2004]. Exceptionally violent rainstorms can overcome orographic barriers and penetrate far into otherwise arid regions in the northwestern Himalayas at elevations above 3000 m [*Bookhagen et al*., 2005]. Otherwise, general blocking effects prevail and penetration occurs along river valleys or mountain passes [*Barros et al*., 2006]. Winter monsoon depressions are either strongly blocked or deflected by topography. Exploratory model simulations show that the implementation of better representation of land-atmosphere interactions at subgrid scales lead to more realistic simulations of precipitation and surface air temperatures [*Dimri*, 2009]. A more accurate representation of resolvable subgrid-scale processes leads to a better simulation of surface latent heat fluxes entering the lower troposphere, which has a strong impact on storm energetics (low-level entropy and convective instability) as well as upslope moisture convergence as demonstrated by *Sun and Barros* [2014]. Using a set of modeling experiments, *Dimri and Niyogi* [2012] provided insight on the interplay of topographic and WD circulations during the 21–23 January 1999 case. In this study longitudinal and vertical cross-sectional distribution of meridional wind and specific humidity at 34°N latitude at 0000 UTC on 21–23 January, respectively, is shown and discussed. This cross section was selected because it contains the highest topographic variability at this latitude. Higher vertical wind shear in the lower troposphere and stronger meridional wind from the surface to 500 hPa along the Kashmir valley (~73°E) is discernible during the WD event. Also, contrast in meridional winds from the surface to 200 hPa is seen around ~67°E. Along the valley walls, the wind is weaker than in the middle of the valley. A corresponding increase in specific humidity up to the midtroposphere over the valley is clearly visible, which is lower along the valley's topographic slopes/boundaries.

To investigate the precipitation mechanisms associated with WDs, a case during 20–22 December 2006 was investigated by *Dimri et al*. [2013], who documented the distribution of moisture variables and orographic vorticity modulation in the intensification of the WD as it interacts with the topography. The Asian Precipitation–Highly Resolved Observational Data Integration Towards Evaluation of the Water Resources (APHRODITE) [*Yatagai et al*., 2012] daily precipitation (24 h cumulative at 0000 UTC on 22 December 2006) indicates that a large event took place (see Figure 8a). The western Himalayan region has a limited observational network, and most of the available reanalyses are based on the assimilation of satellite measurements, upper air observations, and limited ground observations. The number of stations per grid cell (25 km resolution) is available for APHRODITE, and this information was used to determine to what extent the gridded precipitation was determined from station data or derived using an interpolation between the stations. The climate over the western Himalayas is colder and drier than that of other Himalayan regions, and therefore, the daily temporal resolution of APHRODITE allows detection of precipitation events that are missed at the monthly time resolution of other data sets.

The simulated precipitation from the Regional Climate Model (RCM)–REMO [*Jacob et al*., 2007] with a spatial resolution of 0.23° (~25 km) to match the APHRODITE resolution is shown in Figure 8b for the 20–22 December 2006 WD event. The model simulation used global ERA-Interim reanalysis data [*Dee et al*., 2011] to supply large-scale boundary conditions. REMO uses the GTOPO30 topography data from the U.S. Geological Survey. The domains were chosen to cover all of India, including the Himalayas. In the model-simulated and corresponding APHRODITE fields, the peak precipitation appears across the Himalayan range, with the output showing the wet bias. The RCM geopotential height field at 850 hPa (Figure 8c) shows a well-defined surface low associated with cyclonic circulation over 33°N, 65°E in the northwest of the western Himalayas 2 days earlier. The system develops on 20 and 21 December 2006 as it moves over the western Himalayas (Figures 8d and 8e), indicating that such systems can be adequately depicted by the RCM. Vertical distribution of anomalous geopotential and specific humidity gets clear influence by the topographic organization, viz., valley floor, upslopes, and downslopes, and is clearly discernible in defining the spatial organization of precipitation. Vertical deflection of flow by the topography results in adiabatic cooling, and if sufficient moisture is available, clouds form and grow eventually leading to precipitation. Convergence on the upslope/windward side, due to decreased velocity through orographic retardation, will deform or slow down the flow, generating midtroposphere positive vorticity at the peak of the storm [*Dimri et al*., 2013]. Higher relative humidity is seen in the regions of positive vorticity. Weaker negative vorticity occurs along the topographic surface toward the windward side, with positive vorticity over the leeward side and over the valley floors. Thus, the effects of stronger valley flows are twofold: first, these stronger valley flows reduce upslope moisture flow by channeling it, and second, the lateral circulations constrained by the valley boundaries provide conditions for developing clouds and precipitation.

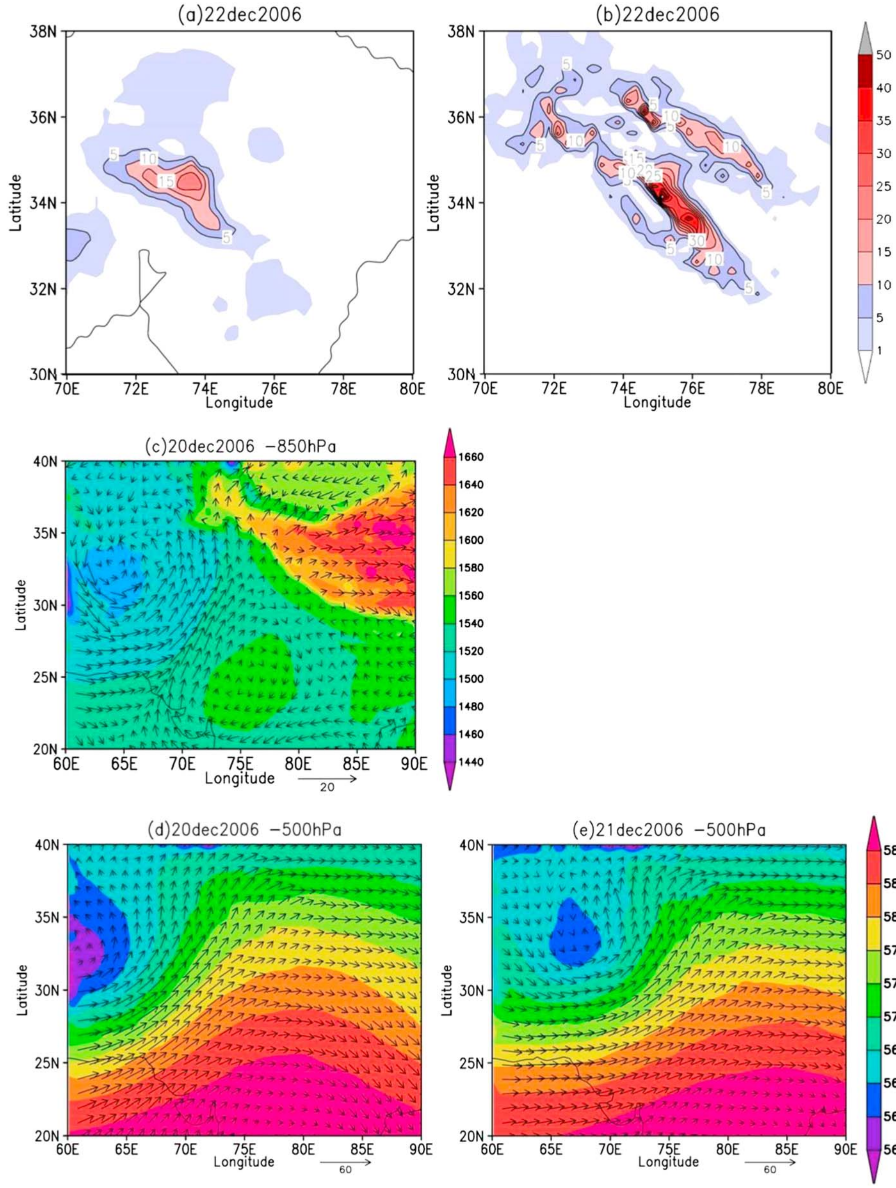

Figure 8. On 22 December 2006, 24 h cumulative precipitation (mm/d) in (a) observational data using the Asian Precipitation–Highly Resolved Observational Data Integration Towards Evaluation of the Water Resources (APHRODITE) [*Yatagai et al*., 2012] and (b) the corresponding Regional Climate Model (RCM)–REMO [*Jacob et al*., 2007] simulated field, and geopotential height (m; shade) and vector wind (m/s; arrow) in the REMO simulation at (c) 850 hPa on 20 December 2006, (d) 500 hPa on 20 December 2006, and (e) 500 hPa on 21 December 2006.

At the mountain range scale, *Smith* [2006] proposed a theoretical framework describing the influence of stable moist airflow on precipitation over mountainous regions. *Roe* [2005] reviewed orographic precipitation processes, in general, emphasizing the notion of storm modification by terrain as a transient phenomenon during the passage of a preexisting weather disturbance over the mountain range, while also being submitted to changes in synoptic conditions, which contrasts with the notion of orographic enhancement from linear theory. A synthesis of current understanding and a comprehensive review of orographic modification of fronts and precipitating weather systems generally including dynamical and microphysical processes were published by *Houze* [2012]. From a modeling perspective, reviews of key orographic precipitation processes including dynamics and microphysics required for skilled simulations were conducted by *Barros and Lettenmaier* [1994], *Leung and Ghan* [1995], *Bindlish and Barros* [2000], and *Lin et al*. [2001] among others. Recent scaling studies suggest unambiguous relationships between the spatial and temporal organization of clouds, precipitation, and convective activity in complex topography that should be useful for the representation of subgrid-scale processes in NWP and climate models [*Nogueira et al.*, 2013; *Nogueira and Barros*, 2014]. Despite increasing success in the simulation of individual storms, operational predictability remains a major challenge with severe shortcomings for hazard response and preparedness in mountainous regions [e.g., *Tao and Barros*, 2013].

8. WDs: Links to Large-Scale Forcing

8.1. Indian Summer Monsoon

The influence of different sections of the Tibetan Plateau (TP) and its orography, referred to as regional mountain uplift, was proposed by *Chakraborty et al.* [2002]. The study suggested that the topography of the western TP is more instrumental to the formation of ISM than the eastern TP. *Boos and Kuang* [2010] illustrated that the presence of the Himalayan orography and its adjacent mountains sustain the present-day strength of ISM. Furthermore, it is the orographic insulation of low entropy, an extratropical air mass by the narrow mountain chains (i.e., thermal insulation), rather than the diabatic heating of the entire elevated plateau that maintains the ISM [*Tang et al.*, 2013].

Anomalous heavy snow in the Himalayas during winter or spring has long been regarded as a possible precursor of deficient Indian monsoon rainfall during the subsequent summer [*Godbole*, 1973; *Hahn and Manabe*, 1975; *Das and Bedi*, 1978; *Yanai et al.*, 1992]. However, the teleconnection mechanisms by which snow anomalies in the Tibetan Plateau affect the summer monsoon and its dependence on the spatial variability of the snowpack remain largely unknown. The Himalayan snow cover during winter is a key factor in long-range forecasting of ISM rainfall [*Vernekar et al.*, 1995; *Dash et al.*, 2004, 2005; *Mamgain et al.*, 2010]. Migration of midlatitude WDs into the tropics leads to weakening of the ISM. Wave kinetic energy associated with these WDs has a significant negative correlation with weekly averaged all India summer rainfall [*Bawiskar et al.*, 2005]. *Bamzai and Shukla* [1999] discussed the connection between Eurasian snow cover and its influences on the upcoming ISM. The relationship between snow cover and the ISM may change in the future as dust and black carbon from anthropogenic sources deposit on the snow and reduce its albedo [*Gautam et al.*, 2013]. A model study by *Turner and Slingo* [2011] highlighted a mechanism involving reduced surface sensible heat and longwave fluxes, reduced heating of the troposphere over the Tibetan Plateau, and a consequently reduced meridional tropospheric temperature gradient that weakens the monsoon during early summer [*Blanford*, 1884; *Fasullo*, 2004]. This is consistent with the work of *Blanford* [1884] who, a century earlier, suggested that winter snow cover over the Himalayas may be an important predictor of subsequent summer precipitation over India. It suggests that dry winds from the mountains would evaporate recent rainfall at lower elevations, so reducing the local moisture for downstream precipitation. In addition, he concluded that a large-scale high-pressure pattern over India could not be attributed to the influence of the Himalayas alone [*Robock et al.*, 2003] This remains an open question. It is referred to here as a counterpoint to the role of Himalayan snow cover. Snow albedo is the key mechanism explaining around 50% of the perturbation in sensible heating over the Tibetan Plateau accounting for the majority of cooling through the troposphere. Various model experiments conducted to understand ISM forecasting on seasonal-to-interannual scales [*Cane*, 1991] produce weak trade winds that result in a heavy winter snowfall regime and a subsequent weak summer monsoon [*Barnett et al.*, 1989].

8.2. Indian Winter Monsoon

Many studies pertaining to the ISM are available whereas very little is known regarding the Indian winter monsoon (IWM). *Rasmusson and Carpenter* [1982] recognized the role of the El Niño phases with the IWM. *Meehl* [1994] connected the evolution of winter and summer upper airflow to Indian subcontinent heating. *Yanai and Li* [1994] investigated the phase relationship between the monsoon index, mean SST of various parts of the equatorial oceans, and Eurasian snow cover and found that snow cover relates to both SST and monsoon index in a quasi-biennial frequency, which is more complicated and suggestive of a two-way interaction. *Kawamura* [1998] explained that due to suppressed convection over the Indonesian region and the symmetric Rossby response due to the attenuated Walker circulation associated with El Niño events, conditions are more conducive for cyclonic circulations over the western Himalayas during wet years (i.e., El Niño years). *Yang et al.* [2002] noted a possible link between the Asian-Pacific-American climate and the East Asian jet stream during boreal winter. During years of high IWM precipitation, a higher magnitude (nearly on the order of magnitude 10) of kinetic energy flux convergence and stronger vorticity generation prevail in comparison to dry years. The resultant surface and upper air fields yield lower sea level pressure and stronger westerly winds over the Saudi Arabian region. The WDs are embedded in the westerlies, and due to the strengthening of these westerlies, strengthening of WDs also occurs [*Dimri*, 2013a]. During years of higher precipitation, middle to upper troposphere shows significant anomalous fields which favor higher frequency and possible intensification of WDs.

Roy [2006] surveyed linkages of IWM with the different phases of ENSO, Pacific Decadal Oscillation (PDO), and local sea surface temperature. The intensification of WDs can be due to a low-pressure trough, which is a dominant feature during positive North Atlantic Oscillation and warm ENSO conditions [*Syed et al*., 2006]. Examination of anomalous kinetic energy balance, vorticity, angular momentum, and the heat and moisture budgets reveals that turbulent exchanges in the middle troposphere result in latent heat release during the IWM; therefore, significant meridional moisture transport from the Arabian Sea to the western Himalayas takes place as a result of the mean motion in the upper troposphere [*Dimri*, 2007].

A positive precipitation anomaly over northwest India is typically found in correspondence to subdued convection over the warm pool region. One proposed mechanism [*Yadav et al*., 2009] is that in abnormally wet years over northwest India, midtropospheric cooling over the warm pool region due to suppressed convection generates an upper level convergence (cyclonic circulation) anomaly over southern Asia that intensifies the westerly jet stream over the Indian region. The Rossby-gyre dynamics with strong vertical and westward meridional tilts in the tropical baroclinic atmosphere form cyclonic circulation anomalies in the upper troposphere due to a weak Madden-Julian Oscillation (MJO) [*Madden and Julian*, 1972] that intensifies the westerly jet stream over the Indian region [*Dimri*, 2013b]. The jet stream guides the WDs, and hence, precipitation increases over northwest India.

9. WDs: In a Changing Climate

The global hydrological cycle is expected to amplify in response to global climate change and variability [*Zahn and Allan*, 2013]. Regions where precipitation is strongly dependent on ocean moisture uptake will experience stronger precipitation events [*Gimeno et al*., 2013]. The variability of midlatitude winter weather is strongly governed by extratropical cyclones, although there is very little evidence that the frequency or wind speed of these cyclones will increase. However, more intense precipitation from the cyclones that carry WDs will have socioeconomic impacts over the western Himalayas, which remains an issue for further investigation in light of existing scientific knowledge and understanding.

Observation-based studies concerning the changing nature of WDs are scarce. *Cannon et al*. [2014] investigated variations and changes in winter WD (WWD) activity from 1970 to 2010 for heavy precipitation events and found significant differences between the western Himalayas and central Himalayan (CH) regions. Specifically, they report an enhancement in the strength and frequency of WWDs with heavy precipitation in the western Himalayas, weakening of the influence of WDs, and decrease in precipitation in the central Himalayas (CH). Based on the Coupled Model Intercomparison Project Phase 3 (CMIP3) experiments, *Meehl et al*. [2007] revealed possible increased future storm activity, while the more recent CMIP5 simulations show a decline in Northern Hemisphere storm activity [*Chang et al*., 2012]. Therefore, what actually matters is the spread in storm trends across the models in both model intercomparisons. If the spread is the same, then the uncertainty has not changed. The depiction of orographically induced snowfall is key to the representation of WD in climate models. Obtaining the correct phase of precipitation requires an adequate representation of the tropospheric profiles of temperature and humidity. Another source of uncertainty is the representation of the regional topography in the coarse-resolution global CMIP series of models. Since polar amplification means that the higher latitudes will warm faster than the Northern Hemisphere as a whole, the latitudinal temperature gradient will decrease [*Hall*, 2004], which should have an impact on total winter snowfall from WDs.

Using consistent but different observational data sets supported by numerical model simulations, *Yadav et al*. [2010] proposed a physical mechanism explaining a potential intensification of WDs in a changing climate. This mechanism suggests a baroclinic response due to the Sverdrup balance related to a large-scale sinking motion over the western Pacific during the warm phase of ENSO. Such a response causes an upper level cyclonic circulation anomaly north of India and a low-level anticyclonic anomaly over southern and central India (as shown by *Dimri and Chevuturi* [2013]). The cyclonic circulation anomaly intensifies the WDs

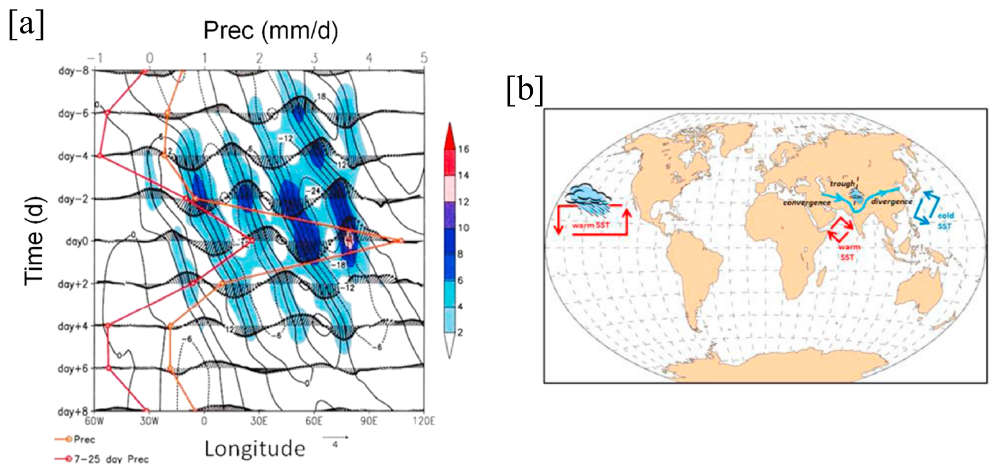

Figure 9. (a) Time-longitude cross-sectional distribution at 35°N latitude of composites for 7–25 days filtered outgoing longwave radiation (W/m^2; color), 500 hPa geopotential height (m; black contour), 500 hPa wind (m/s; arrow), and precipitation (mm/d; red curve; upper *x* axis) anomalies from day −8 to day +8 based on western Himalayan daily precipitation. Day 0 corresponds to the active peak of 7–25 days western Himalayan daily precipitation variation. The orange curve corresponds to anomalous precipitation (mm/d; orange curve; upper *x* axis) from day −8 to day +8 based on western Himalayas daily precipitation and [*Dimri*, 2013b]. Twenty-eight winters (December 1979, January 1980, and February 1980 to December 2006, January 2007, and February 2007) data of height and wind are taken from National Centers for Environmental Prediction/ National Center for Atmospheric Research reanalysis data sets [*Kanamitsu et al.*, 2002]; long-term satellite observations of outgoing longwave radiation (OLR) is taken from the U.S. National Oceanic and Atmospheric Administration (NOAA) [*Liebmann and Smith*, 1996]; precipitation data are used from the Asian Precipitation–Highly Resolved Observational Data Integration Towards Evaluation of the Water Resources (APHRODITE) [*Yatagai et al.*, 2012] to study the ISOs associated with the Indian winter monsoon over the western Himalayas. (b) Schematic representation of physical mechanism associated with enhanced Indian winter monsoon during El Niño phases [*Dimri*, 2013a].

passing over northwest India. With specific reference to the frequency of WDs, *Ridley et al*. [2013] provided a comprehensive overview on the projected increased frequency of WDs up to the year 2100. Due to circulation changes within regional climate model simulations (HadRM3), increased WD occurrences result in an overall 37% increase in winter snowfall [*Ridley et al*., 2013]. This model environment produces higher circulations corresponding to WD evolution and higher precipitation. *Madhura et al*. [2014] also report an increase in WD frequency due to midtropospheric warming trends observed in recent decades over west-central Asia. Such warming will increase the baroclinic instability of the mean westerly wind and could favor increased variability of the WDs and increased precipitation. Another important justification for such an increase is based on the elevation dependency of the climatic signals over the Tibetan Plateau and Himalayan region, which introduces zonally asymmetric changes in the winter circulation through middle and upper tropospheric temperature changes over the Eurasian region. However, using past climate behavior from tree ring analysis, *Yadav* [2011] suggest that in the monsoon shadow zone in the central Himalayas, WD frequency should decrease during spring (March, April, May, and June) in possible response to global-scale teleconnections. These findings question whether the intensification of WD activity will be limited only to winter seasons or if it could spill over to spring and summertime as well.

Future changes of ISM and IWM intensities will have an important effect on Himalayan glaciers [*Moors et al*., 2011]. Winter WD precipitation provides critical mass input to glaciers and snowpack [*Moors and Stoffel*, 2013]. In the spring, snowpack melt provides essential runoff to the regional river networks and to replenish groundwater storage at low elevations. While it seems that increasing air temperatures in the future will push the beginning of the melt season to earlier in the year, and glaciers in headwater basins of the Ganges appear to be on a continued decline, it is not clear whether snowmelt runoff will continue to increase in the future since this depends on the snow accumulation regime of WDs [*Bolch et al*., 2012], which independent of WD intensification may change due to complex changes in the regional energy budget [*Wiltshire*, 2014]. For example, intermittent snowpack melting due to surface warming in the winter may result from increased cloudiness [*Shekhar et al*., 2010].

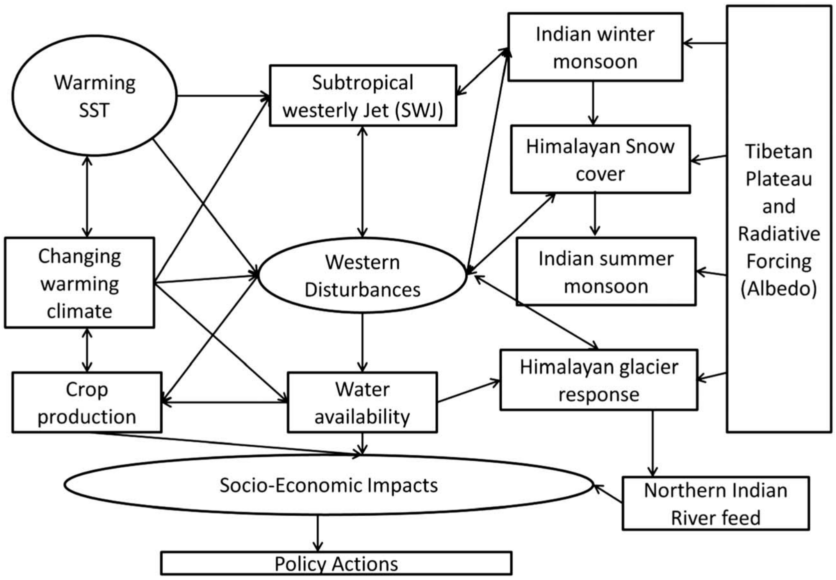

Figure 10. A conceptual framework that shows how WDs relate to other large-scale global, regional, and local processes, along with impacting socioeconomic influences that fit into the climate policy framework.

10. Summary and Synthesis

WDs are important synoptic weather systems that are responsible for almost one third of the annual precipitation over the northern Indian region and most of the cold season precipitation. Understanding these systems is of great socioeconomic importance as they impact glacier mass balance, winter agriculture, water resources, and river hydrology in the northern Indian and Pakistan regions. This manuscript chronologically reviews the evolution of scientific understanding of WDs and related climate and hydrometeorological processes leading to the current state of the knowledge.

Primarily, WDs move periodically as a "family" of evolving, intensifying, and decaying disturbances—a wave train of alternating anomalous anticyclonic and cyclonic circulations. Figure 9a shows time travel composites based on 28 years of data (1980–2008) for active WD peak phases including outgoing longwave radiation, 500 hPa geopotential height, wind, and precipitation anomalies using a 7–25 day pass filter. The traveling wave of outgoing longwave radiation anomalies corresponds to convection, which starts building up approximately 6 days prior to peaking for each WD (day 0). The corresponding wave of anomalous 500 hPa heights depicts the same temporal pattern of WD intensification starting 6–4 days before reaching the maximum. Note the symmetrical phase movement associated with each WD in the 500 hPa wind field. Each WD peaked in the same phase of the 500 hPa wind. Associated precipitation is highest on day 0, and the temporal distribution follows the pattern of WD evolution and decay. This baroclinic structure is a dominant mechanism for storm intensification [*Dimri*, 2013b].

During El Niño events, the warming over the equatorial central/eastern Pacific and Indian Ocean creates conditions that favor the attenuation of the Walker circulation, which in turn facilitates the southward displacement of the SWJ to move southward [*Kawamura*, 1998; *Dimri*, 2013a]. Additionally, consistent with the Rossby-type response in the atmosphere, significant cooling over the eastern Pacific Ocean drives a north-south gradient [*Webster et al.*, 1998] that supports the intensification of the IWM over the western Himalayas (Figure 9b) and results in anomalous WD evolution in the western Himalayas. Finally, increased convection over the tropical Indian Ocean and anomalous WDs over the western Himalayas cooperate to strengthen the Hadley circulation. In such conditions, large-scale meridional transport due to ascending atmospheric motion over the tropical Indian Ocean and descending motion over the western Himalayas region is established. This coupling provides a moisture intake pathway from the southern latitudes that injects substantial moisture to the anomalous WDs, thus increasing precipitation. The vertical baroclinic response over the Himalayan region provides a more suitable condition for genesis/intensification of cyclonic storms (Figure 9a) during wet conditions [*Kawamura*, 1998]. That is, the baroclinic response supports the intensification of WDs and hence the increase of the associated precipitation during wet years. This physical mechanism also promotes the southward shifting of the SWJ over southern Asia associated with the deepening of northwesterly flow in areas immediately west of northern India. Such situations are conducive for enhanced cold surges. As discussed earlier, the attenuated Walker circulation associated with El Niño conditions along with the strengthened Hadley circulation due to asymmetric meridional upper tropospheric flow from the Southern to the Northern Hemisphere work in tandem to push the SWJ southward and provide moisture to present WDs. Such stationary wave phase formation in the midtroposphere provides suitable conditions for genesis/intensification of WDs/troughs. The vertical structure from the lower to upper troposphere strengthens the formation of such synoptic weather, resulting in higher precipitation over the western Himalayas. Nevertheless, further research is needed of the leading/lagging relationship between the Walker and Hadley circulations and IWM, between the IWM and Tibetan Plateau cooling and heating, and of extratropical influences on WD dynamics which may be strongly affected by climate change.

An integrated framework for examining the role of WDs in the context of regional climate and socioeconomic impacts is summarized in Figure 10. A conceptual framework associated with the role of WDs with its plausible interlinks leading to policy framework is provided in Figure 10. It illustrates the role of WDs linking global processes translated to regional and local impacts that in turn motivate policy. High-resolution model assessments investigating WD interactions with topography and land-surface heterogeneities will continue to be important in understanding the different mechanisms that contribute to the temporal evolution of the families of WD storms at regional scale and to understand the complex spatial and temporal variability of precipitation and associated weather at scales relevant for hazard mitigation and decision making.

Acknowledgments
This paper was conceived by A.P.D. and D.N. A.P.D., A.P.B., D.N., and D.R.S. synthesized and prepared this manuscript. Other contributors provided inputs at various stages during the preparation of the manuscript. The authors would like to acknowledge Dallas Staley and Gianna Hartman for providing multiple English writing edits. are due to Mausam for allowing reproduction of Figure 2. The authors also thank the reviewers and the Editor for their constructive guidance, comments, and suggestions that have helped shape this review. D.N. acknowledges support from the NSF CAREER award. Authors would like to acknowledge the use of NCEP data set for analyzing various fields in the present manuscript and as the initial and boundary conditions as input for the model simulation (http://www.esrl.noaa.gov/psd/data/gridded/data.ncep.reanalysis.html). Authors acknowledge the Global Modeling and Assimilation Office (GMAO) and the GES DISC for the dissemination of MERRA data set (http://gmao.gsfc.nasa.gov/research/merra/). Authors also acknowledge *Yatagai et al.* [2012] for using APHRODITE precipitation data sets (http://www.chikyu.ac.jp/precip/). Interpolated OLR data used in the study are provided by the NOAA/OAR/ESRL PSD, Boulder, Colorado, USA (http://www.esrl.noaa.gov/psd/data/gridded/data.interp_OLR.html)

The Editor on this paper was Alan Robock. He thanks Peter Webster and two anonymous reviewers for their assistance in reviewing this manuscript.

References

Academica Sinica (1957), On the general circulation over Eastern Asia (I), *Tellus*, *9*, 432–446.
Agnihotri, C. L., and M. S. Singh (1982), Satellite study of Western Disturbances, *Mausam*, *33*(2), 249–254.
Agrawal, K. C. (1999), An introduction of avalanche forecasting and future trends, in *The Himalayan Environment*, edited by S. K. Dash and J. Bhadur, pp. 71–78, New Age International Pvt. Ltd, New Delhi.
Ananthakrishnan, R., and R. N. Keshavmurty (1973), A preliminary study of the adiabatic generation and dissipation of kinetic energy by meridional and zonal winds over India and neighborhood during winter seasons, *Indian J. Meteorol. Geophys.*, *24*, 235–244.
Anders, A. M., G. H. Roe, B. Hallet, D. R. Montgomery, N. J. Finnegan, and J. Putkonen (2006), Spatial patterns of precipitation and topography in the Himalaya, in *Tectonics, Climate, and Landscape Evolution*, *Geol. Soc. of Am. Spec. Pap*., vol. 398, edited by S. D. Willett et al., pp. 39–53, Geol. Soc. of Am., Boulder, Colo.
Azadi, M., U. C. Mohanty, O. P. Madan, and B. Padmanabhamurty (2001), Prediction of precipitation associated with Western Disturbances using a high-resolution regional model: Role of parameterisation of physical processes, *Meteorol. Appl.*, *7*, 317–326.
Azadi, M., U. C. Mohanty, and O. P. Madan (2005), Performance of a limited area model for the simulation of Western Disturbances, *J. Aerosp. Sci. Tech.*, *2*(2), 29–35.
Bamzai, A. S., and J. Shukla (1999), Relation between Eurasian snow cover, snow depth and the Indian summer monsoon: An observational study, *J. Clim.*, *12*, 3117–3132.
Bannon, J. K. (1954), Note on the structure of the high altitude strong-wind belt in the Middle East in winter, *Q. J. R. Meteorol. Soc.*, *80*(344), 218–221.
Barnett, T. P., L. Dümenil, U. Schlese, E. Roeckner, and M. Latif (1989), The effect of Eurasian snow cover on regional and global climate variations, *J. Atmos. Sci.*, *46*, 661–685.
Barros, A. P., and D. P. Lettenmaier (1994), Dynamic modeling of orographically-induced precipitation, *Rev. Geophys.*, *32*, 265–284, doi:10.1029/94RG00625.
Barros, A. P., J. Putkonen, and D. W. Burbank (2000), A study of 1999 monsoon rainfall in a mountainous region in central Nepal using TRMM products and rain gauge observations, *Geophys. Res. Lett.*, *27*, 3683–3686, doi:10.1029/2000GL011827.
Barros, A. P., G. Kim, E. Williams, and S. W. Nesbitt (2004), Probing orographic controls in the Himalayas during monsoon using satellite imagery, *Nat. Hazards Earth Syst. Sci.*, *4*, 29–51.
Barros, A. P., S. Chiao, T. J. Lang, D. Burbank, and J. Putkonen (2006), From weather to climate—Seasonal and interannual variability of storms and implications for erosion processes in the Himalaya, in *Tectonics, Climate, and Landscape Evolution: Geological Society of America Special Paper*, *Penrose Conf. Ser*., vol. 398, edited by S. D. Willett et al., pp. 17–28, Geol. Soc. of Am., Boulder, Colo.
Bawiskar, S. M., M. D. Chipade, V. R. Mujumdar, and P. V. Puranik (2005), Kinetic energy of extratropical waves and their effect on the Indian monsoon rainfall, *Mausam*, *56*(3), 337–342.
Bhattacharya, B. K., K. R. Gunjal, S. Panigrahy, and J. S. Parihar (2011), Albedo-rainfall feedback over Indian Monsoon region using long term observations between 1981 to 2000, *J. Indian Soc. Remote Sens.*, *39*(3), 393–406.
Bindlish, R., and A. P. Barros (2000), Disaggregation of rainfall for one way coupling of atmospheric and hydrological models in regions of complex terrain, *Global Planet. Change*, *25*, 111–132.
Blanford, H. F. (1884), On the connexion of the Himalaya snowfall with dry winds and seasons of draught in India, *Proc. R. Soc. London*, *37*, 1–23.
Bolch, T., et al. (2012), The state and fate of Himalayan glaciers, *Science*, *336*(6079), 310–314.
Bookhagen, B., R. C. Thiede, and M. R. Strecker (2005), Abnormal monsoon years and their control on erosion and sediment flux in high, arid northwest Himalaya, *Earth Planet. Sci. Lett.*, *231*, 131–146.

Boos, W. R., and Z. Kuang (2010), Dominant control of the South Asian monsoon by orographic insulation versus plateau heating, *Nature*, *463*, 218–222.

Bugayev, V. A., V. A. Giorgio, E. M. Kozik, M. A. Petrosyants, A. J. Pshenitshnij, N. N. Romanov, and O. N. Tshernysheva (1957), *Synoptic Processes of Central Asia* [in Russian], 477 pp., Publishing Company of the Academy of Sciences of the Usbek Soviet Republic, Tashkent.

Cane, M. A. (1991), Forecasting El Niño with a geophysical model, in *Teleconnections Connecting World-Wide Climate Anomalies*, edited by M. Glantz, R. Katz, and N. Nicholls, Chap. 11, pp. 345–369, Cambridge Univ. Press, New York.

Cannon, F., L. M. V. Carvalho, C. Jones, and B. Bookhagen (2014), Multi-annual variations in winter westerly disturbance activity affecting the Himalaya, *Clim. Dyn.*, *44*, 441–455, doi:10.1007/s00382-014-2248-8.

Chakraborty, A., R. S. Nanjundiah, and J. Srinivasan (2002), Role of Asian and African orography in Indian summer monsoon, *Geophys. Res. Lett.*, *29*(20), 1989, doi:10.1029/2002GL015522.

Chakravarti, A. K. (1968a), Summer rainfall in India: A review of monsoonal and extramonsoonal aspects – I, *Atmosphere*, *6*(1), 21–28.

Chakravarti, A. K. (1968b), Summer rainfall in India: A review of monsoonal and extramonsoonal aspects – II, *Atmosphere*, *6*(3), 87–114.

Chang, E. K. M., Y. Guo, and X. Xia (2012), CMIP5 multimodel ensemble projection of storm track change under global warming, *J. Geophys. Res.*, *117*, D23118, doi:10.1029/2012JD018578.

Chanysheva, S. G., O. I. Subbotina, U. V. Petrov, E. T. Egamberdiyev, B. A. Aizensh-tat, and G. N. Leukhina (1995), *Variability of the Central Asian Climate* [in Russian], 215 pp., Central Asian Hydrometeorological Research Institute, Tashkent, Russia.

Charney, J. G. (1947), The dynamics of long waves in a baroclinic westerly current, *J. Meteorol.*, *4*, 135–162.

Charney, J. G. (1948), On the scale of atmospheric motions, *Geofys. Publ.*, *17*(2), 1–17.

Charney, J. G., R. Fjørtoft, and J. Von Neumann (1950), Numerical integration of the barotropic vorticity equation, *Tellus*, *2*, 237–254.

Chaudhury, A. M. (1950), On the vertical distribution of wind and temperature over Indo-Pakistan along the meridian 76°E in winter, *Tellus*, *2*(1), 56–62.

Chitlangia, P. R. (1976), Mean model of western depression, *Indian J. Meteorol. Hydrol. Geophys.*, *87*(2), 157–162.

Das, P. K., and H. S. Bedi (1978), Inclusion of Himalayas in a PE model, *Indian J. Meteorol. Hydrol. Geophys.*, *29*, 373–383.

Das, S. (2002), Evaluation and verification of MM5 forecasts over the Indian region, 2005 MM5 Workshop. [Available at www.mmm.ucar.edu/mm5/workshop/ws02/Das.pdf/url>.]

Das, S. (2005), Mountain weather forecasting using MM5 modelling system, *Curr. Sci.*, *88*(6), 899–905.

Das, S., S. V. Singh, E. N. Rajagopal, and R. Gall (2003), Mesoscale modeling for mountain weather forecasting over the Himalayas, *Bull. Am. Meteorol. Soc.*, *84*(9), 1237–1244.

Das, S., R. Ashrit, and M. W. Moncrieff (2006), Simulation of a Himalayan cloudburst event, *J. Earth Syst. Sci.*, *115*(3), 299–313.

Dasgupta, M., S. Das, and R. Ashrit (2012), MM5 3D-Var data assimilation and forecast system over Indian Subcontinent—Results from recent experiments. [Available at http://www.mmm.ucar.edu/mm5/workshop/ws04/Session5/Gupta.Das.pdf.]

Dash, S. K., and B. Chakrapani (1989), Simulation of a winter circulation over India using global spectral model, *Earth Planet. Sci.*, *98*(2), 189–205.

Dash, S. K., G. P. Singh, A. D. Vernekar, and M. S. Shekhar (2004), A study on the number of snow days over Eurasia, Indian rainfall and seasonal circulations, *Meteorol. Atmos. Phys.*, *86*, 1–13.

Dash, S. K., G. P. Singh, M. S. Shekhar, and A. D. Vernekar (2005), Response of the Indian summer monsoon circulation and rainfall to seasonal snow depth anomaly over Eurasia, *Clim. Dyn.*, *24*, 1–10.

Datta, R. K., and M. G. Gupta (1967), Synoptic study of the formation and movements of western depressions, *Indian J. Meteorol. Geophys.*, *18*(1), 45–50.

Dee, D. P., et al. (2011), The ERA-Interim reanalysis: Configuration and performance of the data assimilation system, *Q. J. R. Meteorol. Soc.*, *137*, 553–597.

Defant, F., and H. Taba (1957), The threefold structure of the atmosphere and the characteristics of the tropopause, *Tellus*, *9*(3), 259–274.

Defant, F., and H. Taba (1958), The breakdown of the zonal circulation during the period January 8 to 13, 1956, the characteristics of temperature field and tropopause and its relation to the atmospheric field of motion, *Tellus*, *10*(4), 430–450.

DeSilva, A. M., and R. S. Lindzen (1993), On the establishment of stationary waves in the Northern Hemisphere winter, *J. Atmos. Sci.*, *50*, 43–61.

Dimri, A. P. (2004), Impact of horizontal model resolution and orography on the simulation of a Western Disturbance and its associated precipitation, *Meteorol. Appl.*, *11*, 115–127.

Dimri, A. P. (2007), The transport of momentum, sensible heat, potential energy and moisture over the western Himalayas during the winter season, *Theor. Appl. Climatol.*, *90*(1–2), 49–63.

Dimri, A. P. (2009), Impact of subgrid scale scheme on topography and land use for better regional scale simulation of meteorological variables over the Western Himalayas, *Clim. Dyn.*, *32*, 565–574.

Dimri, A. P., U. C. Mohanty, and M. Mandal (2004), Simulation of heavy precipitation associated with an intense western disturbance over northwest Himalayas, *Nat. Hazards*, *31*(2), 499–519.

Dimri, A. P., U. C. Mohanty, M. Azadi, and L. S. Rathore (2006), Numerical study of western disturbances over western Himalayas using mesoscale model, *Mausam*, *57*(4), 579–590.

Dimri, A. P. (2013a), Interannual variability of Indian Winter Monsoon over the Western Himalaya, *Global Planet. Change*, *106*, 39–50.

Dimri, A. P. (2013b), Intraseasonal oscillation associated with the Indian winter monsoon, *J. Geophys. Res. Atmos.*, *118*, 1–10, doi:10.1002/jgrd.50144.

Dimri, A. P., and A. Chevuturi (2013), Model sensitivity analysis study for Western Disturbances over the Himalayas, *Meteorol. Atmos. Phys.*, *1-26*, 155–180.

Dimri, A. P., and D. Niyogi (2012), Regional climate model application at subgrid scale on Indian winter monsoon over the western Himalayas, *Int. J. Climatol.*, *23*, 2185–2205, doi:10.1002/joc3584.

Dimri, A. P., and U. C. Mohanty (2009), Simulation of mesoscale features associated with intense Western Disturbances over western Himalayas, *Meteorol. Appl.*, *16*, 289–308.

Dimri, A. P., T. Yasunari, A. Wiltshire, P. Kumar, C. Mathison, J. Ridley, and D. Jacob (2013), Application of regional climate models to the Indian winter monsoon over the western Himalayas, *Sci. Total Environ.*, doi:10.1016/j.scitotenv.2013.01.040.

Duan, A., and G. Wu (2005), Role of the Tibetan Plateau thermal forcing in the summer climate patterns over subtropical Asia, *Clim. Dyn.*, *24*, 793–807.

Endlich, R. M., and G. S. McLean (1957), The structure of the jet stream core, *J. Meteorol.*, *14*, 543–552.

Fasullo, J. (2004), A stratified diagnosis of the Indian monsoon-Eurasian snow cover relationship, *J. Clim.*, *17*(5), 1110–1122.

Flohn, H. (1968), *Contribution to a Meteorology of the Tibetan Highlands*, *Atmos. Sci. Pap.*, vol. 130, 120 pp., Dept. of Atmos. Sci., Colo. State Univ., Fort Collins.

Ganju, A., and A. P. Dimri (2004), Prevention and mitigation of avalanche disasters in Western Himalayan region, *Nat. Hazards*, *31*, 357–371.

Gautam, R., N. C. Hsu, W. K. M. Lau, and T. J. Yasunari (2013), Satellite observations of desert dust-induced Himalayan snow darkening, *Geophys. Res. Lett.*, *40*, 988–993, doi:10.1002/grl.50226.

Gimeno, L. R., R. Nieto, A. Drumond, R. Castillo, and R. Trigo (2013), Influence of the intensification of the major oceanic moisture sources on continental precipitation, *Geophys. Res. Lett.*, *40*, 1443–1450, doi:10.1002/grl.50338.

Godbole, R. V. (1973), Numerical simulation of the Indian summer monsoon, *Indian J. Meteorol. Geophys.*, *24*, 1–14.

Gregory, D., and P. R. Rowntree (1990), A mass flux convection scheme with representation of cloud ensemble characteristics and stability-dependent closure, *Mon. Weather Rev.*, *118*, 1483–1506.

Gupta, A., L. S. Rathore, S. V. Singh, and N. Mendiratta (1999), Performance of a global circulation model in predicting the winter systems and associated precipitation over North West India during 1994–97, in *The Himalayan Environment*, edited by S. K. Dash and J. Bahadur, pp. 123–138, New Age Publ., New Delhi, India.

Gupta, S. C., and G. S. Mandal (1987), Behaviour of kinetic energy generation function during a Western Disturbance in May 1982, *Mausam*, *38*(1), 97–102.

Hahn, D. G., and S. Manabe (1975), The role of mountains in the south Asian monsoon circulation, *J. Atmos. Sci.*, *32*(8), 1515–1541.

Hall, A. (2004), The role of surface albedo feedback in climate, *J. Clim.*, *17*(7), 1550–1568.

Hatwar, H. R., B. P. Yadav, and Y. V. R. Rao (2005), Prediction of Western Disturbances and associated weather over Western Himalayas, *Curr. Sci.*, *88*(6), 913–920.

Hoskins, B. J., and D. J. Karoly (1982), The steady linear response of a spherical Atmosphere to thermal and Orographic forcings, *J. Atmos. Sci.*, *38*, 1179–1196.

Houghton, J. T. (1987), Importance of satellites for weather forecasting, *Nature*, *326*, 450–450, doi:10.1038/326450a0.

Houze, R. A., Jr. (2012), Orographic effects on precipitating clouds, *Rev. Geophys.*, *50*, RG1001, doi:10.1029/2011RG000365.

Jacob, D., et al. (2007), An inter-comparison of regional climate models for Europe: Model Performance in present day climate, *Clim. Change*, *81*, 31–52.

Kalsi, S. R., and S. R. Halder (1992), Satellite observations of interaction between tropics and mid-latitudes, *Mausam*, *43*(1), 59–64.

Kanamitsu, M., W. Ebisuzaki, J. Woollen, S.-K. Yang, J. J. Hnilo, M. Fiorino, and G. L. Potter (2002), NCEP–DOE AMIP-II Reanalysis (R-2), *Bull. Am. Meteorol. Soc.*, *83*(11), 1631–1643.

Kawamura, R. (1998), A possible mechanism of the Asian summer monsoon-ENSO coupling, *J. Meteorol. Soc. Jpn.*, *76*, 1009–1027.

Koteswaram, P. (1957a), Mean zonal wind circulation over India, *Indian J. Meteorol. Geophys.*, *8*, 346.

Koteswaram, P. (1957b), *Meteorological in Relation to High Level Aviation*, pp. 101–108, Indian Meteorol. Dept. Publ., New Delhi, India.

Koteswaram, P., and S. Parathasarathy (1954), The mean jet stream over India in the pre-monsoon and post-monsoon seasons and vertical motions associated with sub-tropical jet streams, *Indian J. Meteorol. Geophys.*, *5*(2), 138–156.

Koteswaram, P., C. R. V. Raman, and S. Parthasarathy (1953), The mean jet stream over India and Burma in winter, *Indian J. Meteorol. Geophys.*, *4*(2), 111–122.

Krishna Kumar, K., B. Rajagopalan, and M. A. Cane (1999), On the weakening relationship between the Indian Monsoon and ENSO, *Science*, *284*(5423), 2156–2159.

Krishna Kumar, K., B. Rajagopalan, M. Hoerling, G. Bates, and M. A. Cane (2006), Unraveling the mystery of Indian monsoon failure during El Niño, *Science*, *314*(5796), 115–119.

Krishnamurti, T. N., A. Kumar, K. S. Yap, A. P. Dastoor, N. Davidson, and J. Sheng (1990), Performance of a high resolution mesoscale tropical prediction model, *Adv. Geophys.*, *32*, 133–286.

Kuang, X., and Y. Zhang (2005), Seasonal variation of the east Asian subtropical westerly jet and its association with the heating fields over East Asia, *Adv. Atmos. Sci.*, *22*, 831–840.

Kucharski, F., A. Bracco, J. H. Yoo, and F. Molteni (2007), Low-frequency variability of the Indian monsoon-ENSO relationship and the tropical Atlantic: The "weakening" of the 1980s and 1990s, *J. Clim.*, *20*(16), 4255–4266.

Lang, T. J., and A. P. Barros (2002), An investigation of the onsets of the 1999 and 2000 monsoons in Central Nepal, *Mon. Weather Rev.*, *130*, 1299–1316.

Lang, T. J., and A. P. Barros (2004), Winter storms in central Himalayas, *J. Meteorol. Soc. Jpn.*, *82*(3), 829–844.

Leung, L. R., and S. J. Ghan (1995), A subgrid parameterization of orographic precipitation, *Theor. Appl. Climatol.*, *52*, 95–118.

Liebmann, B., and C. Smith (1996), Description of a complete (interpolated) outgoing longwave radiation dataset, *Bull. Am. Meteorol. Soc.*, *77*, 1275–1277.

Lin, Y.-L., S. Chiao, T.-A. Wang, M. L. Kaplan, and R. P. Weglarz (2001), Some common ingredients for heavy orographic rainfall, *Weather Forecasting*, *16*, 633–660.

Liu, X., and M. Yanai (2002), Influence of Eurasian spring snow cover on Asian summer rainfall, *Int. J. Climatol.*, *22*, 1075–1089.

Madden, R. A., and P. R. Julian (1972), Description of global scale circulation cells in the tropics with a 40–50 day period, *J. Atmos. Sci.*, *29*, 1109–1123.

Madhura, R. K., R. Krishnan, J. V. Revadekar, M. Mujumdar, and B. N. Goswami (2014), Changes in Western Disturbances over the western Himalayas in a warming environment, *Clim. Dyn.*, *44*, 1157–1168, doi:10.1007/s00382-014-2166-9.

Malurkar, S. L. (1947), Abnormally dry and wet Western Disturbances over North India, *Curr. Sci.*, *16*(5), 139–141.

Mamgain, A., S. K. Dash, and P. P. Sarthi (2010), Characteristics of Eurasian snow depth with respect to Indian summer monsoon rainfall, *Meteorol. Atmos. Phys.*, *110*(1), 71–83.

Meehl, G. A. (1994), Coupled ocean-atmosphere-land processes and south Asian monsoon variability, *Science*, *256*, 263–267.

Meehl, G. A., C. Covey, T. Delworth, M. Latif, B. McAvaney, J. F. B. Mitchell, R. J. Stouffer, and K. E. Taylor (2007), The WCRP CMIP3 multi-model dataset: A new era in climate change research, *Bull. Am. Meteorol. Soc.*, *88*, 1383–1394.

Mohanty, U. C., O. P. Madan, P. L. S. Rao, and P. V. S. Raju (1998), Meteorological fields associated with Western Disturbances in relation to glacier basins of western Himalayas during winter season, Tech. Rep., Centre for Atmospheric Science, IIT Delhi, India.

Mohanty, U. C., O. P. Madan, P. V. S. Raju, R. Bhatla, and P. L. S. Rao (1999), A study on certain dynamic and thermodynamic aspects associated with Western Disturbances over north-west Himalaya, in *The Himalayan Environment*, edited by S. K. Dash and J. Bhadur, pp. 113–122, New Age International Pvt. Ltd, New Delhi.

Mohri, K. (1953), On the fields of wind and temperature over Japan and adjacent waters during winter of 1950–1951, *Tellus*, *5*(3), 340–358.

Mohri, K. (1958), Jet streams and upper fronts in the general circulation and their characteristics over the Far East. Part. I, *Geophys. Mag.* (Tokyo), *29*, 45–126.

Montgomery, R. B. (1940), Report on the work of G. T. Walker, *Mon. Weather Rev.* (Supplement), *39*, 26.

Mooley, D. A. (1957), The role of Western Disturbances in the production of weather over India during different seasons, *Indian J. Meteorol. Geophys.*, *8*(3), 253–260.

Moors, E. J., and M. Stoffel (2013), Changing monsoon patterns, snow and glacial melt, its impacts and adaptation options in northern India: Synthesis, *Sci. Total Environ.*, *468*, S162–S167.
Moors, E. J., et al. (2011), Adaptation to changing water resources in the Ganges basin, northern India, *Environ. Sci. Policy*, *14*(7), doi:10.1016/j.envsci.2011.03.005.
Mull, S., and B. N. Desai (1947), The origin and structure of the winter depression of Northwest India India Meteorological Department, Technical Note No. 25:18.
Murray, R. (1953), Jet stream over the British isles during June 14–18, 1951, *Meteorol. Mag.*, *82*, 971.
Nakamura, H. (1992), Midwinter suppression of baroclinic wave activity in the Pacific, *J. Atmos. Sci.*, *49*, 1629–1642.
Newton, C. W., and A. V. Persson (1962), Structural characteristics of the subtropical jet stream and certain lower-stratospheric wind systems, *Tellus*, *14*(2), 221–241.
Nigam, S., and R. S. Lindzen (1989), The sensitivity of stationary waves to variations in the basic state zonal flow, *J. Atmos. Sci.*, *46*, 1746–1768.
Nogueira, M., and A. P. Barros (2014), The non-convective/convective structural transition in stochastic scaling of atmospheric fields, *J. Geophys. Res. Atmos.*, *119*, 13,771–13,794, doi:10.1002/2014JD022548.
Nogueira, M., A. P. Barros, and P. Miranda (2013), Multifractal properties of embedded convective structures in orographic precipitation: Toward subgrid-scale predictability, *Nonlinear Processes Geophys.*, *20*, 1–17, doi:10.5194/npg-20-1-2013.
Pisharoty, P., and B. N. Desai (1956), Western Disturbances and Indian weather, *Indian J. Meteorol. Geophys.*, *7*, 333–338.
Puranik, D. M., and R. N. Karekar (2009), Western Disturbances seen with AMSU-B and infrared sensors, *J. Earth Syst. Sci.*, *118*(1), 27–39.
Raju, P. V. S., R. Bhatla, and U. C. Mohanty (2011), A study on certain aspects of kinetic energy associated with Western Disturbances over northwest India, *Atmósfera*, *24*(4), 375–384.
Rakesh, V., R. Singh, D. Yliya, P. K. Pal, and P. C. Joshi (2009), Impact of variational assimilation of MODIS thermodynamic profiles in the simulation of Western Disturbance, *Int. J. Remote Sens.*, *30*(18), 4867–4887.
Ramanathan, Y., and K. R. Saha (1972), Application of a primitive equation barotropic model to predict movement of Western Disturbances, *J. Appl. Meteorol.*, *11*, 268–272.
Ramasastri, K. S. (1999), Snow melt modeling studies in India, in *The Himalayan Environment*, edited by S. K. Dash and J. Bahadur, pp. 59–70, New Age International, New Delhi, India.
Ramaswamy, C. (1956), On the sub-tropical jet stream and its role in the development of large-scale convection, *Tellus*, *8*(1), 26–60.
Ramaswamy, C. (1962), Breaks in the Indian summer monsoon as a phenomenon of interaction between the easterly and the sub-tropical westerly jet streams, *Tellus*, *14*(3), 337–349.
Ramaswamy, C. (1966), The problem of fronts in Indian atmosphere, *Indian J. Meteorol. Geophys.*, *17*(2), 151–170.
Rangachary, N., and B. K. Bandyopadhyay (1987), An analysis of the synoptic weather pattern associated with extensive avalanching in Western Himalaya, *IAHS Publ.*, *162*, 311–316.
Rao, N. S. B., and P. E. Moray (1971), Cloud systems associated with Western Disturbances: A preliminary study, *Indian J. Meteorol. Geophys.*, *22*, 413–420.
Rao, V. B., and S. T. Rao (1971), A theoretical and synoptic study of Western Disturbances, *Pure Appl. Geophys.*, *90*(7), 193–208.
Rao, Y. P., and V. Srinivasan (1969), Discussion of typical synoptic weather situation: Winter Western Disturbances and their associated features Indian Meteorological Department: Forecasting Manual Part III.
Rasmusson, E. M., and T. H. Carpenter (1982), Variations in tropical sea surface temperature and surface wind fields associated with the Southern Oscillation/El Niño, *Mon. Weather Rev.*, *110*(5), 354–384.
Ridley, J., A. Wiltshire, and C. Mathison (2013), More frequent occurrence of westerly disturbances in Karakoram up to 2100, *Sci. Total Environ.*, doi:10.1016/j.scitotenv.2013.03.074.
Riehl, H. (1962), Jet streams of the atmosphere, Colorado State Univ., Tech. Pap., 32.
Riehl, H., M. A. Alaka, C. L. Jordan, and R. J. Renard (1954), *The Jet Stream*, Meteorological Monographs, vol. 2, Am. Meteorol. Soc., Boston, Mass.
Rienecker, M. M., et al. (2011), MERRA: NASA's Modern-Era Retrospective Analysis for Research and Applications, *J. Clim.*, *24*, 3624–3648.
Robock, A., M. Mingquan, Y. V. Konstantin, and D. Robinson (2003), Land surface conditions over Eurasia and Indian summer monsoon rainfall. *J. Geophys. Res.*, *108*(D4), 4131, doi:10.1029/2002JD002286.
Roe, G. H. (2005), Orographic precipitation, *Ann. Rev. Earth Planet. Sci.*, *33*, 645–671.
Roy, S. S. (2006), The impacts of ENSO, PDO, and local SSTs on winter precipitation in India, *Phys. Geogr.*, *27*(5), 464–474.
Roy, S. S., and S. K. R. Bhowmik (2005), Analysis of the thermodynamics of the atmosphere over northwest India during the passage of a Western Disturbance as revealed by model analysis field, *Curr. Sci.*, *88*(6), 947–951.
Saha, S. K., S. Halder, K. Krishna Kumar, and B. N. Goswami (2011), Pre-onset land surface processes and 'internal' interannual variabilities of the Indian summer monsoon, *Clim. Dyn.*, *36*, 2077–2089.
Schiemann, R., D. Luthi, and C. Schar (2009), Seasonality and interannual variability of the westerly jet in the Tibetan Plateau region, *J. Clim.*, *22*, 2940–2957.
Semwal, G., and R. K. Giri (2007), Precipitation simulation of synoptic scale systems over western Himalayan region using Advanced Regional Prediction System (ARPS) model, *Mausam*, *58*(4), 471–480.
Semwal, G., and A. P. Dimri (2012), Impact of initial and boundary conditions on simulations of western disturbances and associated precipitation, *Nat. Hazards*, *64*(2), 1405–1424.
Serebreny, S. M., E. J. Wiegman, and R. G. Hadfield (1962), Some characteristic features of the jet stream complex during selected synoptic conditions, *J. Appl. Meteorol.*, *1*(2), 137–153.
Sharma, R. V., and D. V. Subramaniam (1983), The Western Disturbance of 22 December 1980: A case study, *Mausam*, *34*(1), 117–120.
Shekhar, M. S., H. Chand, S. Kumar, K. Srinivasan, and A. Ganju (2010), Climate-change studies in the western Himalaya, *Ann. Glaciol.*, *51*(54), 105–112.
Singh, M. S. (1963), Upper air circulation associated with a Western Disturbance, *Indian J. Meteorol. Geophys.*, *14*, 156–172.
Singh, M. S. (1971), Study of the jet stream over India and to its north in winter: Part II, *Indian J. Meteorol. Geophys.*, *22*, 149–160.
Singh, M. S. (1980), Tropospheric structure and jet-streams over the Middle-East in winter, *Mausam*, *31*(2), 241–246.
Singh, M. S., and S. Kumar (1977), Study of Western Disturbance, *Indian J. Meteorol. Hydrol. Geophys.*, *28*(2), 233–242.
Singh, M. S., A. V. R. K. Rao, and S. C. Gupta (1981), Development and movement of a mid-tropospheric cyclone in the westerlies over India, *Mausam*, *32*(1), 45–50.
Smith, R. B. (1979), The influence of the mountains on the atmosphere, *Adv. Geophys.*, *21*, 87–230, doi:10.1016/S0065-2687(08)60262-9.
Smith, R. B. (2006), Progress on the theory of orographic precipitation, *Spec. Pap. Geol. Soc. Am.*, *398*, 1–16.
Srinivasan, K., A. Ganju, and S. S. Sharma (2005), Usefulness of mesoscale weather forecast for avalanche forecasting, *Curr. Sci.*, *88*(6), 921–926.

Srinivasan, V. (1971), Some case studies of cirriform clouds over India during the winter period, *Indian J. Meteorol. Geophys.*, *22*, 421–428.

Sun, X., and A. P. Barros (2014), Isolating the Role of surface evapotranspiration on moist convection and cloud formation along the eastern flanks of the Andes using a quasi-idealized approach, *J. Atmos. Sci.*, *72*, 243–261, doi:10.1175/JAS-D-14-048.

Syed, F. S., F. Giorgi, J. S. Pal, and M. P. King (2006), Effect of remote forcings on the winter precipitation of central southwest Asia. Part 1: Observations, *Theor. Appl. Climatol.*, *86*(1), 147–160.

Tang, H., A. Micheels, J. S. Eronen, B. Ahrens, and M. Fortelius (2013), Asynchronous responses of East Asian and Indian summer monsoons to mountain uplift shown by regional climate modeling experiments, *Clim. Dyn.*, *40*, 1531–1549.

Tao, J., and A. P. Barros (2013), Prospects for flash flood forecasting in mountainous regions—An investigation of Tropical Storm Fay in the Southern Appalachians, *J. Hydrol.*, *506*, 69–89, doi:10.1016/j.jhydrol.2013.02.052.

Thayyen, R. J., A. P. Dimri, P. Kumar, and G. Agnihotri (2012), Study of cloudburst and flash floods around Leh, India during August 4–6, 2010, *Nat. Hazards*, *65*, 2175–2204, doi:10.1007/s11069-012-0464-2.

Thomas, L., S. K. Dash, and U. C. Mohanty (2013), Influence of various land surface parameterization schemes on the simulation of the Western Disturbances, *Meteorol. Appl.*, *21*, 635–643, doi:10.1002/met.1386.

Tiedtke, M. (1989), A comprehensive mass flux scheme for cumulus parameterization in large-scale models, *Mon. Weather Rev.*, *117*, 1779–1800.

Turner, A. G., and J. M. Slingo (2011), Using idealized snow forcing to test teleconnections with the Indian summer monsoon in the Hadley Centre GCM, *Clim. Dyn.*, *36*, 1717–1735.

Veeraraghavan, K., and T. Nath (1989), A satellite study of an active Western Disturbance, *Mausam*, *40*(3), 303–306.

Venkiteshwaran, S. P. (1939), Rainfall due to winter disturbances and the associated upper air temperatures over Agra, *Proc. Natl. Inst. Sci. India*, *5*(1), 117–121.

Vernekar, A. D., J. Zhou, and J. Shukla (1995), The effect of Eurasian snow cover on the Indian monsoon, *J. Clim.*, *8*, 248–266.

Walker, G. T. (1924), Correlation in seasonal variation of weather. X: Application to seasonal forecasting in India Mem. Indian Meteorol. Dept., 24, 333±345.

Webster, P. J., V. O. Magana, T. N. Palmer, J. Shukla, R. A. Tomas, M. Yanai, and T. Yasunari (1998), Monsoons: Processes, predictability, and the prospects for prediction, *J. Geophys. Res.*, *103*, 14,451–14,510, doi:10.1029/97JC02719.

Wiltshire, A. J. (2014), Climate change implications for the glaciers of the Hindu Kush, Karakoram and Himalayan region, *Cryosphere*, *8*(3), 941–958.

Wu, G. and Y. Liu (2003), Summertime quadruplet heating patterns in the subtropics and the associated atmospheric circulation, *Geophys. Res. Lett.*, *30*(5), 1201, doi:10.1029/2002GL016209.

Yadav, R. K., K. RupaKumar, and M. Rajeevan (2009), Increasing influence of ENSO and decreasing influence of AO/NAO in the recent decades over northwest India winter precipitation, *J. Geophys. Res.*, *114*, D12112, doi:10.1029/2008JD011318.

Yadav, R. K., J. H. Yoo, F. Kucharski, and M. A. Abid (2010), Why is ENSO influencing northwest India winter precipitation in recent decades?, *J. Clim.*, *23*(8), 1979–1993.

Yadav, R. R. (2011), Long-term hydroclimatic variability in monsoon shadow zone of western Himalaya, India, *Clim. Dyn.*, *36*(7-8), 1453–1462.

Yanai, M., and C. Li (1994), Interannual variability of the Asian summer monsoon and its relationship with ENSO, Eurasian snow cover and heating, in *Proceedings of the International Conference on Monsoon Variability and Prediction, WMO/TD 619*, vol. I, pp. 27–34, World Meteorological Organization, Geneva, Switzerland.

Yanai, M., C. Li, and Z. Song (1992), Seasonal heating of the Tibetan Plateau and its effects on the evolution of the Asian summer monsoon, *J. Meteorol. Soc. Jpn.*, *70*, 319–351.

Yang, S., K. M. Lau, and K. M. Kim (2002), Variations of the East Asian jet stream and Asian-Pacific-American winter climate anomalies, *J. Clim.*, *15*(3), 306–325.

Yatagai, A., K. Kamiguchi, O. Arakawa, A. Hamada, N. Yasutomi, and A. Kitoh (2012), APHRODITE: Constructing a long-term daily gridded precipitation dataset for Asia based on a dense network of rain gauges, *Bull. Am. Meteorol. Soc.*, *93*, 1401–1415, doi:10.1175/BAMS-D-11-00122.1.

Zahn, M., and R. P. Allan (2013), Climate warming-related strengthening of the tropical hydrological cycle, *J. Clim.*, *26*, 562–574, doi:10.1175/JCLI-D-12-00222.1.